1998

# Thermodynamic Constraints on Nitrogen Transformations and Other Biogeochemical Processes at Soil-Stream Interfaces

Lars O. Hedin
*Cornell University*

Joseph C. von Fischer
*Cornell University*

Nathaniel E. Ostrom
*Michigan State University*

Brian P. Kennedy
*Dartmouth College*

Michael G. Brown
*Cornell University*

*See next page for additional authors*

*Ecology*, 79(2), 1998, pp. 684–703


# THERMODYNAMIC CONSTRAINTS ON NITROGEN TRANSFORMATIONS AND OTHER BIOGEOCHEMICAL PROCESSES AT SOIL–STREAM INTERFACES

LARS O. HEDIN,[1] JOSEPH C. VON FISCHER,[1] NATHANIEL E. OSTROM,[2] BRIAN P. KENNEDY,[3] MICHAEL G. BROWN,[1] AND G. PHILIP ROBERTSON[4]

[1]*Section of Ecology and Systematics, Cornell University, Ithaca, New York 14853 USA*
[2]*Department of Geological Sciences, Michigan State University, East Lansing, Michigan 48824 USA*
[3]*Department of Biology, Dartmouth College, Hanover, New Hampshire, USA*
[4]*W. K. Kellogg Biological Station and Department of Crop and Soil Sciences, Michigan State University, Hickory Corners, Michigan 49083, USA*

*Abstract.* There is much interest in biogeochemical processes that occur at the interface between soils and streams since, at the scale of landscapes, these habitats may function as control points for fluxes of nitrogen (N) and other nutrients from terrestrial to aquatic ecosystems. Here we examine whether a thermodynamic perspective can enhance our mechanistic and predictive understanding of the biogeochemical function of soil–stream interfaces, by considering how microbial communities interact with variations in supplies of electron donors and acceptors. Over a two-year period we analyzed >1400 individual samples of subsurface waters from networks of sample wells in riparian wetlands along Smith Creek, a first-order stream draining a mixed forested–agricultural landscape in southwestern Michigan, USA. We focused on areas where soil water and ground water emerged into the stream, and where we could characterize subsurface flow paths by measures of hydraulic head and/or by in situ additions of hydrologic tracers.

We found strong support for the idea that the biogeochemical function of soil–stream interfaces is a predictable outcome of the interaction between microbial communities and supplies of electron donors and acceptors. Variations in key electron donors and acceptors ($NO_3^-$, $N_2O$, $NH_4^+$, $SO_4^{2-}$, $CH_4$, and dissolved organic carbon [DOC]) closely followed predictions from thermodynamic theory. Transformations of N and other elements resulted from the response of microbial communities to two dominant hydrologic flow paths: (1) horizontal flow of shallow subsurface waters with high levels of electron donors (i.e., DOC, $CH_4$, and $NH_4^+$), and (2) near-stream vertical upwelling of deep subsurface waters with high levels of energetically favorable electron acceptors (i.e., $NO_3^-$, $N_2O$, and $SO_4^{2-}$).

Our results support the popular notion that soil–stream interfaces can possess strong potential for removing dissolved N by denitrification. Yet in contrast to prevailing ideas, we found that denitrification did not consume all $NO_3^-$ that reached the soil–stream interface via subsurface flow paths. Analyses of subsurface N chemistry and natural abundances of $\delta^{15}N$ in $NO_3^-$ and $NH_4^+$ suggested a narrow near-stream region as functionally the most important location for $NO_3^-$ consumption by denitrification. This region was characterized by high throughput of terrestrially derived water, by accumulation of dissolved $NO_3^-$ and $N_2O$, and by low levels of DOC. Field experiments supported our hypothesis that the sustained ability for removal of dissolved $NO_3^-$ and $N_2O$ should be limited by supplies of oxidizable carbon via shallow flowpaths. In situ additions of acetate, succinate, and propionate induced rates of $NO_3^-$ removal ($\sim$1.8 g $N \cdot m^{-2} \cdot d^{-1}$) that were orders of magnitude greater than typically reported from riparian habitats. We propose that the immediate near-stream region may be especially important for determining the landscape-level function of many riparian wetlands. Management efforts to optimize the removal of $NO_3^-$ by denitrification ought to consider promoting natural inputs of oxidizable carbon to this near-stream region.

*Key words: denitrification; field experiment; hydrologic flow-paths; microbial metabolism; nitrogen; nitrogen retention; nitrogen transformations; nitrous oxide; riparian zone; soil–stream interface; thermodynamic constraints on biogeochemical processes; wetlands.*

## INTRODUCTION

The question of how nutrients and elements move within heterogeneous landscapes is of fundamental importance to ecology (Pickett and Cadenasso 1995). Knowledge of mechanisms that control magnitudes and paths of nutrient flux between different ecosystems translates directly into better ways to predict and manage effects of human activities within landscapes. Such knowledge is also of basic importance because it helps

Manuscript received 7 August 1996; revised 15 March 1997; accepted 7 April 1997.

ecologists understand how ecosystem processes are coupled at the scale of entire landscapes. Of particular interest are habitats that display disproportionately high rates of biogeochemical activity. Such habitats can serve as ''control points'' within landscapes by affecting the amounts and/or forms of nutrients that are transported along paths of nutrient flux.

The soil–stream interface is perhaps the most obvious and important control point along paths of nutrient flux from terrestrial to aquatic ecosystems (e.g., Lowrance et al. 1984*a*, *b*, Peterjohn and Correll 1984, Jacobs and Gilliam 1985*a*, *b*, Cooper 1990, Groffman et al. 1991, McDowell et al. 1992, Triska et al. 1993*a*, *b*, Hanson et al. 1994, Jansson et al. 1994, Hill 1996). Biogeochemical transformations at this interface can affect the degree to which processes in terrestrial ecosystems are translated into changes in the chemistry of surface waters. This unique biogeochemical importance of soil–stream interfaces results from the interaction of two key properties: an unusually high potential for biogeochemical transformations in near-stream riparian wetlands (e.g., Lowrance et al. 1984*b*, Cooper 1990, Bowden et al. 1992, Lloyd 1993, Triska et al. 1993*a*, *b*), and the interception and rapid throughput of water and nutrients from the surrounding terrestrial watershed (e.g., Freeze and Cherry 1979, Hill 1991, Hill and Waddington 1993). In fact, soil–stream interfaces are within many watersheds positioned so that terrestrially derived water necessarily passes through this interface before emerging as surface water (Likens et al. 1977).

Over the past two decades there has been much interest in how biogeochemical processes that occur at soil–stream interfaces within riparian wetlands can act to reduce or ''buffer'' losses of N from terrestrial to aquatic ecosystems (e.g., Lowrance et al. 1984*b*, Peterjohn and Correll 1984, Jacobs and Gilliam 1985*a*, *b*, Warwick and Hill 1988, Cooper 1990, Groffman et al. 1991, McDowell et al. 1992, Simmons et al. 1992, Haycock and Pinay 1993, Jordan et al. 1993, Paterson and Schnoor 1993, Triska et al. 1993*a*, *b*, Hanson et al. 1994, Jansson et al. 1994, Vought et al. 1994, Groffman et al. 1996). Improved knowledge about these processes holds the prospect of better management of landscapes, which, in turn, could lead to reduced diffuse-source inputs of N to surface waters from agricultural, urban, and atmospheric pollution sources.

Several processes can retain or remove N as subsurface water flows through soil–stream interfaces. Plant uptake and/or microbial immobilization is often thought to be of lesser long-term significance since biotic N pools become saturated over time and since immobilized N is eventually re-released to solution by microbial mineralization (but see Paterson and Schnoor 1993, Pinay et al. 1995). Dissolved N can be lost in gaseous forms (as NO and $N_2O$) during nitrification in soils (e.g., Firestone and Davidson 1989, Bowden et al. 1992, Matson and Vitousek 1995), but this process is also not a likely long-term buffer of N losses because it is invariably associated with strong production of hydrologically mobile $NO_3^-$—a form of N that is readily lost to downstream ecosystems (see Hedin 1994, Holmes et al. 1994). More attention has focused on microbial denitrification since this process in theory can yield strong and sustained transformations of dissolved N into gaseous forms (mainly as $N_2$ and $N_2O$) within wetland environments, as long as conditions remain favorable for the appropriate microbial communities (Lloyd 1993).

Field studies have generally supported the idea of soil–stream interfaces as potential control points for N transformations within landscapes. Rates of actual and potential denitrification can be exceptionally high in anoxic environments at soil–stream interfaces (e.g., Cooper 1990, Bowden et al. 1992, Lowrance 1992, Schipper et al. 1993, Hanson et al. 1994, Pinay et al. 1995) and can be accompanied by strong reductions in $NO_3^-$ along subsurface flow paths (Bowden et al. 1992, Pinay et al. 1993, 1995). Some studies have furthermore demonstrated that soil–stream interfaces can remove substantial amounts of $NO_3^-$ that is added experimentally in the field (Groffman et al. 1991, 1996). Regional-scale evidence comes from a recent study of large watersheds in North America and Europe, in which Howarth et al. (1996) found that the majority ($\sim$75%) of N inputs by atmospheric deposition and fertilizer could not be accounted for by hydrologic outputs in rivers. Howarth et al. conclude that such imbalances in the N budget might reflect, in addition to some limited retention of N in aggrading forest areas, that substantial quantities of N are lost via denitrification processes in habitats such as riparian wetlands.

Yet, strong N removal is by no means a universal property of soil–stream interfaces. Hill (1996) notes that N transformations vary considerably among different soil–stream interfaces, with many examples of weak to non-existent removal of dissolved N (also see Warwick and Hill 1988, Devito et al. 1989, Correll 1991, Hill 1991, Phillips et al. 1993, Jacks et al. 1994, Jones and Holmes 1996) and in some cases even net production of $NO_3^-$ due to nitrification processes (cf. Holmes et al. 1994, Jones et al. 1995*a*). Two recent reviews (Hill 1996, Jones and Holmes 1996) have argued that our ability to predict the extent to which different soil–stream interfaces can function to buffer N flux depends on better understanding of how biogeochemical processes are linked to hydrologic properties such as water flow paths. However, such understanding has been difficult to develop, to a great degree because soil–stream interfaces often are exceptionally variable environments for both microbial and hydrologic processes (e.g., Grimm and Fisher 1984, Jones and Holmes 1996). For example, the chemistry of subsurface soil waters and ground waters can change several-fold over distances of less than a few meters (Hill 1990, Dahm et al. 1991, Hendricks and White 1991,

TABLE 1. Sequence of microbial redox reactions, arranged according to decreasing yield of free energy for conditions of decreasing (A) vs. increasing (B) p$\mathcal{E}$ (cf. Fig. 1). Energies are calculated per mole available organic matter for reduction reactions (A) and per mole $O_2$ for oxidation reactions (B). $\triangle G^{0\prime} = \triangle G^0 - R \times T \times \ln[H^+]^C$, where pH = 7 and $C$ = stoichiometric coefficient for $H^+$, and other reactants are at 1 mol/L.

| Process | Reaction | Free energy (kJ) |
|---|---|---|
| A) Decreasing p$\mathcal{E}$ | | |
| (1) Aerobic respiration | $CH_2O + O_2 \rightarrow CO_2 + H_2O$ | −501 |
| (2) Denitrification | $CH_2O + (4/5)NO_3^- + (4/5)H^+ \rightarrow CO_2 + (2/5)N_2 + (7/5)H_2O$ | −476 |
| (3) Sulfate reduction | $CH_2O + (1/2)SO_4^{2-} + (1/2)H^+ \rightarrow (1/2)HS^- + H_2O + CO_2$ | −102 |
| (4) Methanogenesis | a) $CH_2O \rightarrow (1/2)CH_4 + (1/2)CO_2$ | −93 |
| | b) $(1/2)CO_2 + 2H_2 \rightarrow (1/2)CH_4 + H_2O$ | −66 |
| B) Increasing p$\mathcal{E}$ | | |
| (5) Methane oxidation | $O_2 + (1/2)CH_4 \rightarrow (1/2)CO_2 + H_2O$ | −408 |
| (6) Sulfide oxidation | $O_2 + (1/2)HS^- \rightarrow (1/2)SO_4^{2-} + (1/2)H^+$ | −399 |
| (7) Nitrification | $O_2 + (1/2)NH_4^+ \rightarrow (1/2)NO_3^- + H^+ + (1/2)H_2O$ | −181 |

*Notes:* G is the Gibbs free energy of a chemical reaction; $G^0$ indicates standard conditions, i.e., 25°C and atmospheric pressure, and the added prime stipulates pH = 7. $R$ is a constant for the number of joules per mole of reaction; $T$ = temperature in degrees Kelvin; $[H^+]^C$ is the molar concentration of hydrogen ions raised to the $C$ power. Adapted from Morel and Hering (1993), Champ et al. (1979), and Stumm and Morgan (1981).

McDowell et al. 1992, Holmes et al. 1994, Groffman et al. 1996). Equally strong variations can be found in microbial processes (Cooper 1990, Bowden et al. 1992, Lowrance 1992, Schipper et al. 1993, Jones 1995, Jones et al. 1995*a*) and in the paths by which subsurface waters moves between soil and stream environments (Hill 1990, Bencala 1993, Harvey and Bencala 1993, Valett et al. 1994, Jones et al. 1995*b*, Hill 1996).

Here we evaluate whether this strong biogeochemical variability can be understood mechanistically by adopting a thermodynamic approach. We consider spatial and temporal variations in water chemistry, hydrology, and stable N isotopes in two riparian wetlands where significant amounts of terrestrially derived water emerged into a stream, and to a lesser degree in nine additional wetlands along the same stream. We base our analysis on a thermodynamic perspective of microbial metabolism: that activities of broad functional groups of microbial populations (e.g., denitrifiers, sulfate reducers, or methanogens) are constrained by patterns of supply of electron donors and acceptors (Stumm and Morgan 1981, Lovely and Phillips 1987, Correll and Weller 1989, Chapelle and Lovely 1992, Morel and Hering 1993). We seek to integrate biogeochemical and hydrologic information by examining how supplies in electron donors and acceptors depend on variations in subsurface flow paths. We focus on understanding N transformations and apply measures of natural $\delta^{15}N$ stable isotope abundances to resolve locations and the relative importance of denitrification vs. nitrification processes. Based on water-chemistry trends we hypothesize that supply of electron donors (as oxidizable DOC [dissolved organic carbon]) ultimately limits removal of N via denitrification; we test this hypothesis by in situ experimental additions of DOC to soil–stream interfaces.

We investigate a specific area within riparian wetlands: the interface between soils and streams (i.e., ''soil–stream interface''). Our studies are based on the idea that soil–stream interfaces that intercept terrestrially derived water are important control points for nutrient flux from terrestrial to aquatic ecosystems. This perspective (cf. McClain et al. 1994) differs importantly from studies that consider nutrient transport in the opposite direction: from stream water into the ''hyporheic zone'' of stream sediments, during which additional biogeochemical transformations can occur (e.g., Grimm and Fisher 1984, Bencala 1993, Harvey and Bencala 1993, Triska et al. 1993*a*, *b*, Findlay 1995, Valett et al. 1995).

### *Thermodynamic constraints on microbial metabolism*

Microbial metabolism depends on the use of electron donors and electron acceptors in redox reactions that generate energy for growth and maintenance (Zehnder and Stumm 1988, Morel and Hering 1993):

$$A_{red} + B_{ox} \rightarrow A_{ox} + B_{red} + \text{free energy} \qquad (1)$$

where $A_{red}$ = electron donor, $B_{ox}$ = electron acceptor, $A_{ox}$ = oxidized form of $A$, $B_{red}$ = reduced form of $B$. While organic matter ($CH_2O$) dominates as the electron donor in many natural environments, other electron donors (e.g., $CH_4$, $HS^-$, Fe(II), $NH_4^+$, and Mn(II)) can be locally important. Similarly, $O_2$ dominates as the electron acceptor in oxic environments, while $NO_3^-$, $N_2O$, Mn(IV), Fe(III), $SO_4^{2-}$, $CO_2$, and $CH_2O$ can be locally important in anoxic environments. Different combinations of electron donors and electron acceptors in Expression 1 release different amounts of free energy that, in turn, can be harnessed for microbial growth and maintenance. For example, aerobic respiration ($CH_2O$ as electron donor, $O_2$ as electron acceptor) generates almost five times more free energy (501 kJ) per mole $CH_2O$ oxidized than does sulfate reduction (102 kJ; $CH_2O$ as electron donor, $SO_4^{2-}$ as electron acceptor) at pH 7 and molar concentrations of reactants (Table 1).

Free energy yields can be used to predict both temporal and spatial patterns of microbial redox reactions

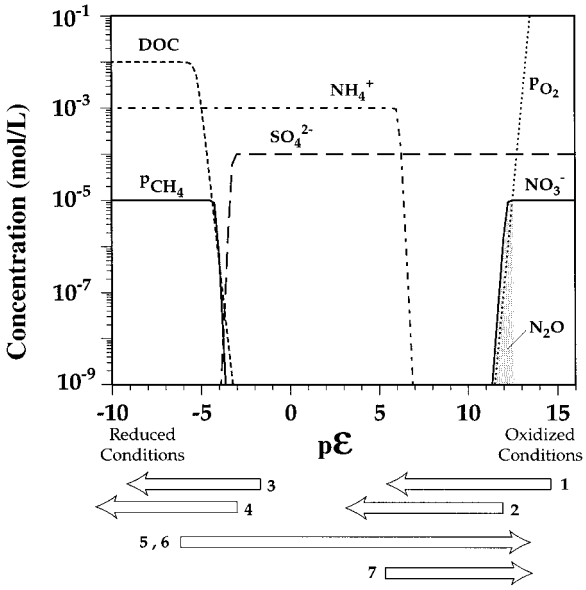


FIG. 1. Predicted thermodynamic equilibrium concentrations of selected electron donors and acceptors as a function of the redox state p$\mathcal{E}$ of the environment at pH 7. [p$\mathcal{E}$ is a measure of the electron activity, which, in turn, is one way to characterize the oxidation state of a system: p$\mathcal{E}$ = $-\log\{e^-\}$. More-negative values indicate a reducing environment or reaction, while more-positive values indicate oxidizing conditions. The expression "p$\mathcal{E}$" shares a similar origin to pH, which is a common measure of the activity of hydrogen ions in a system: pH = $-\log\{H^+\}$.] DOC = dissolved organic carbon; $P_{O_2}$ and $P_{CH_4}$ are partial pressures. Concentration lines are based on the following reactions from Table 1: $O_2$ = aerobic respiration (1) in system open to atmosphere; $NO_3^-$ = denitrification to $N_2$ (2) with $[NO_3^-] + 2 \times [N_2] = 10^{-5}$ mol/L; $SO_4^{2-}$ = sulfate reduction (3) with $[SO_4^{2-}] + [HS^-] = 10^{-4}$ mol/L; $CH_4$ = product of methane fermentation (4) with $[CH_4] + [CO_2] = 10^{-5}$ mol/L; $NH_4^+$ = nitrification (7) with $[NH_4^+] + [NO_3^-] = 10^{-3}$ mol/L; DOC = oxidation of succinate to $CO_2$ with $\Sigma$ C = $10^{-2}$ mol/L. Numbered arrows indicate approximate regions for these reactions, and for sulfide oxidation (5) and methane oxidation (6) in natural environments. The shaded area indicates the approximate region for transient $N_2O$ accumulation during denitrification (Tiedje 1988). These ideal predictions may not always be realized in natural environments due to nonequilibrium conditions or variations in concentrations of reactants and products. Adapted in part from Stumm and Morgan (1981).

in natural habitats (Stumm and Morgan 1981, Lovely and Phillips 1987, Chapelle and Lovely 1992, Morel and Hering 1993). Such thermodynamically based predictions depend on the assumption that, in a given environment, the metabolic reaction that yields most energy will dominate over any competing reactions (e.g., Zehnder and Stumm 1988, Morel and Hering 1993). While the mechanistic reason for such competitive exclusion is not entirely clear, it appears that microbes that can extract energy at higher rates from their environment also are better competitors (higher affinity and/or greater maximal rate of consumption) for limited supplies of electron donors or electron acceptors (Kristjansson and Schönheit 1983, Robinson and Tiedje 1984, Lovely and Phillips 1987, Chapelle and Lovely 1992).

In Fig. 1 we show how microbial processes, and concentrations of selected nutrients and elements, are predicted to change as a function of redox state of the environment, expressed as p$\mathcal{E}$. From the progressive decrease in energy yield of different electron acceptors we expect the following sequence as an environment becomes increasingly reduced due to microbial consumption of electron acceptors (i.e., p$\mathcal{E}$ decreases from right to left in Fig. 1): (1) Loss of $O_2$ (aerobic respiration); (2) loss of $NO_3^-$ (denitrification); (3) loss of $SO_4^{2-}$ (sulfate reduction); and (4) accumulation of $CH_4$ (methane fermentation). We have not explicitly considered Mn and Fe since our study focuses on nitrogen, carbon, and sulfur. Conversely, as an environment becomes increasingly oxidized (i.e., p$\mathcal{E}$ increases from left to right in Fig. 1), we expect the following sequence: (5) Loss of $CH_4$ (methane oxidation); (6) accumulation of $SO_4^{2-}$ (sulfate oxidation); (7) loss of $NH_4^+$ and accumulation of $NO_3^-$ (nitrification). The approximate regions of the different microbial reactions are identified by arrows in Fig. 1 (adapted from Stumm and Morgan 1981).

This sequence of change in chemistry (Fig. 1) applies to many freshwater and soil environments but is not universally applicable because energy yields depend not only on the form of electron donors and acceptors (Table 1) but also on the concentrations of reactants and products in Expression 1. For example, sulfate reducers may not always out-compete methanogens in environments with high pH, high sulfide, and very low concentrations of sulfate (Morel and Hering 1993; also see Howarth 1993), yet such conditions are not relevant for this study (Lovely and Klug 1983). It is difficult from a practical perspective to clearly separate methane oxidation from sulfide oxidation because both reactions have very close energy yields (Table 1), which makes the relative location of these processes in Fig. 1 sensitive to variations in local chemical conditions. It is also difficult to derive exact predictions for trends in dissolved organic carbon (DOC) in Fig. 1 because DOC is a summary measure of various forms of dissolved organic molecules that differ in propensity to donate electrons. Nevertheless since DOC acts as the dominant electron donor for many of the processes depicted in Fig. 1 (Table 1) we expect an overall trend of decreasing DOC concentrations as the environment becomes more oxidized (left to right in Fig. 1), as indicated by DOC in the form of succinate in Fig. 1.

### *Specific predictions*

We used Fig. 1 to derive thermodynamically based predictions of variations in electron donors and acceptors within soil–stream interfaces. To understand N transformations we focused on forms of dissolved inorganic N ($NO_3^-$, $NH_4^+$, and $N_2O$), on organic electron

donors (DOC), and on competing electron acceptors ($SO_4^{2-}$ and methanogenesis; our data on $O_2$ are limited). We evaluated the following predictions along the redox gradient from near-stream oxidized to inland reduced environments (right to left in Fig. 1): (1) $NO_3^-$ decreases before $SO_4^{2-}$ decreases; (2) $NO_3^-$ decreases before $NH_4^+$ increases; (3) $NO_3^-$ decreases before DOC increases; (4) $N_2O$ decreases before $SO_4^{2-}$ decreases; (5) $N_2O$ decreases before DOC increases; and (6) $SO_4^{2-}$ decreases before $CH_4$ increases. Our statistical approach is outlined below in *Methods and site description.*

## Methods and Site Description

### *Study area*

Our study sites were located along Smith Creek, a first-order stream in the Augusta Creek drainage basin of southwestern Michigan, USA (Hedin and Brown 1994). The land use of the surrounding landscape is varied and includes agriculture, pasture, oldfields, woodlands, and wetlands. Our study sites are dominated by sedges and grasses, and are surrounded by oak–hickory forest. The area is underlain by thick deposits of glacial till and outwash, and streamwater chemistry is strongly influenced by the weathering of sandstone, shale, and limestone. The water of Smith Creek is hard, basic (pH range: 7.6–8.5; $n = 32$ sample dates), and contains significant amounts of sulfate (4.5–15.6 mg/L; $n = 70$ sample dates), chloride (2.1–4.8 mg/L; $n = 71$ sample dates) and base cations (Hedin and Brown 1994). While Smith Creek drains mainly second-growth forests and wetlands, agricultural areas are present within the topographic drainage basin.

Houghton muck soils dominate along Smith Creek and well-drained Oshtemo sandy loam soils are common in upland areas. We found near-stream soils to consist of a highly organic upper horizon (0–5 cm, ~20% C), a mixed organic–inorganic sand horizon (5–60 cm, 2–15% C), and a deeper inorganic sand horizon (>60 cm). The top organic horizon contained mainly fine (<0.5 mm) organic particles with low C:N ratios (ratio = 13.9 ± 0.7 [mean ± 1 SD]; $n = 13$ soil samples), apparently derived from aged and well-decomposed organic matter. Below the organic horizon was alluvially deposited sand with low clay content to a depth of at least 100 cm. We interpret this overall horizontal zonation to reflect sand and organic matter deposited by recent fluvial activity (5–60 cm depth), underlain by sand with little or no organic matter deposited by Pleistocene fluvio-glacial processes.

### *Well and piezometer transects*

Installation of shallow wells along transects from inland to near-stream environments permitted us to sample subsurface water as it moved across the soil–stream interface. We installed well transects at 11 different sample areas along the stream. Nine of these areas were in hydrologically ''gaining'' reaches; that is, they showed net influx of water from the soil to the stream. We focused our more detailed chemical and hydrologic studies on two riparian wetland areas with strong influx of soil- and ground water into the stream, and which we developed more extensively into ''well fields'' by installing networks of permanent wells over ~8–12 $m^2$ of soil area. Field 1 consisted of 5 parallel transects of 6 wells, each transect spanning 4 m perpendicularly across the soil–stream interface (Fig. 2A). Because of weak gradients in water tables along the stream we were able to sample water within specific

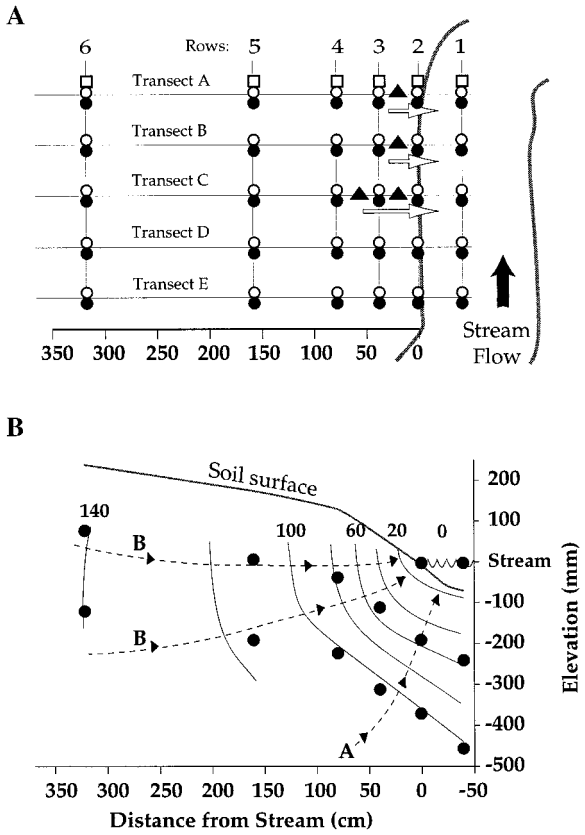


FIG. 2. (A) Location of sample wells in Field 1 at the soil–stream interface of Smith Creek, Michigan, USA. Wells sampled subsurface water at three depths below the soil–sediment surface: 20 cm (●), 40 cm (○), and 100 cm (□). The wells also served as piezometers for measurement of hydraulic head relative to a reference point. ▲ = locations of additions of $Br^-$ hydrologic tracer and DOC. Open arrows indicate dominant paths of horizontal flow of subsurface waters, based on hydrologic tracer information. The vertical scale is same as the horizontal scale (i.e., the transects are 50 cm apart). (B) Cross-sectional distribution of average hydraulic head (in millimeters) at the soil–stream interface of Field 1 in Smith Creek, Michigan, USA, on 5 August 1993 ($n = 5$ transects). Solid lines indicate equipotentials, and dashed lines indicate dominant flow paths: near-stream upwelling of deeper ground water (A) and lateral inflow of shallow subsurface water (B). Location of piezometers is indicated by (●). Note difference in scales between horizontal and vertical axes.

strata by placing inlet ports at depths measured below the soil surface; ports at 20 and 40 cm depth captured water moving through the mixed organic–inorganic horizon (5–60 cm depth) and at 100 cm depth captured water in the deeper inorganic horizon (>60 cm depth). Wells had average inlet port depths (depth at which sample is collected; see below) at 20 cm ($n = 30$), 40 cm ($n = 30$) and 100 cm ($n = 6$) below the soil or sediment surface of Field 1. Field 2, located 14 m downstream and on the opposite side of the stream from Field 1, consisted of 4 transects of 6 wells spanning 3.5 m across the soil–stream interface, with inlet ports at 40 cm depth below the soil or sediment surface. Field 3 was located 38 m upstream of Field 1 and consisted of two transects of 5 wells at 20 cm depth. An additional eight sample areas, each consisting of single transects of 4–6 wells at depths between 20 and 30 cm, were located at 3, 22, 52, 108, 171, and 183 m upstream and at 5 and 17 m downstream of Field 1.

The nested design of Field 1 provided detailed horizontal and vertical chemical, isotopic, and hydrologic information, and we sampled seven dates during the summer of 1993 (3363 separate chemical analyses of 601 individual water samples). In addition to isotopic and hydrologic information, Field 2 provided an extended record of subsurface water chemistry over 38 dates from October of 1991 to October of 1993 (3469 analyses of 693 samples). Field 3 and the eight additional transects furnished only limited chemical and hydrologic information during the summer of 1993 (1–3 sample events; 424 analyses of 126 samples). In addition, Field 1 was the site of experimental DOC additions (see *Experimental carbon additions*, below) and both Fields 1 and 2 received experimental $Br^-$ additions to trace flow paths (Fig. 2A).

We constructed wells from 19 mm (inner diameter [ID]) polyvinyl chloride PVC pipes with inlet ports made from a series of 3-mm-diameter holes located over a 10-cm-deep area at the bottom end of the pipe. The wells extended 20–30 cm below the inlet port to ensure collection of sufficient sample volume after wells were purged (described below). We could also use these wells as piezometers for measures of hydraulic head relative to a permanent reference point (Freeze and Cherry 1979) since they were sealed except for at the inlet port. We installed wells with a sharpened steel tube corer and minimized contamination from organic soil horizons by shielding well pipes inside a second, clean, steel tube as they were lowered into position. Wells were in firm contact with surrounding soils and sediments and were capped by rubber stoppers between sample events.

### *Sampling and analysis of solutes and gases*

This study covers 2 yr of chemical sampling (6 November 1991–29 October 1993) at varying frequencies depending on dissolved constituents, season, and whether samples were associated with any experimental treatment. Before sampling we purged each well using a hand-operated pump to allow fresh subsurface water to enter the bottom of the well. Water samples were withdrawn using polypropylene syringes and tygon tubing (~3.1-mm ID), were filtered immediately through pre-rinsed Gelman A/E glass fiber filters (<1 μm nominal pore size, tested in our laboratory), stored in polyethylene bottles, and kept on ice until refrigerated (generally <3 h). Sample bottles, syringes, filter holders, and tubing were acid washed and leached with excess deionized water. The most sensitive non-gaseous solutes ($NH_4^+$, $NO_3^-$, DON, and DOC) were analyzed within a few days, and were only at rare occasions refrigerated up to 3 wk before analysis. Tests in our laboratory showed that, when filtered immediately in the field, non-gaseous solutes were stable for >3 wk in capped and refrigerated sample bottles. Sulfate, $Cl^-$, $NO_3^-$, and $Br^-$ were analyzed on a Dionex Ion Chromatograph using chemically suppressed conductivity detection and a Dionex AS4A column. Ammonium and Si were analyzed by Alpkem automated colorimetry (Alpkem 1992*a*, *b*); pH by potentiometry using a Ross electrode (Analytical Technology, San Diego, California, USA); DOC by Ionics (Watertown, Massachusetts, USA) high-temperature (850°C) platinum-catalyst combustion; DON by high-temperature (120°C) persulfate digestion with subsequent analysis of $NO_3^-$ by cadmium reduction colorimetry (Alpkem 1992*c*; modified from McDowell et al. 1987 and D'Elia et al. 1977). Persulfate digestion efficiency was tested against amino acid, $NO_3^-$, and $NH_4^+$ standards and by ensuring that all detectable DOC was digested, using a post-digestion DOC analysis as described above. Method detection limits were: $NO_3^-$-N, <0.002 mg/L; $NH_4^+$-N, <0.001 mg/L; DON, <0.01 mg/L; DOC, <0.1 mg/L; $Br^-$, <0.002 mg/L. For concentrations below these limits, we assigned a value of half the detection limit.

We modified the syringe method to collect water for dissolved $N_2O$ and $CH_4$ analysis. We used a smaller diameter (2.3-mm ID) sample tube to minimize losses of gas that might occur across the air–water interface of the leading edge of sample water in the sample tube. Our laboratory tests with solutions of saturated concentrations of $N_2O$ and $CH_4$ showed that, after complete expulsion of ambient air from this syringe-tube system, three rinses with 5 mL of sample was sufficient to prohibit any significant (at $P < 0.05$; $t$ test) loss of $N_2O$ or $CH_4$. In the field we used 10-mL polypropylene syringes that were connected to sample tubes and rinsed (3 times, with 5 mL) before the collection of each 5-mL sample. Syringes were sealed by three-way nylon Pharmaseal valves, transported on ice in a cooler, equilibrated to room temperature in the laboratory, and analyzed within 4 h from the time of sampling. Linear-regression analysis showed no significant loss in $N_2O$ (at 8.2 μL/L: $P > 0.22$; $n = 10$) or $CH_4$ (at 180 μL/L: $P > 0.26$; $n = 18$) from syringes during 5 h of storage in our laboratory environment. In the laboratory we

added 5 mL of nitrogen gas head space to the syringes, shook vigorously for ~2 min, and analyzed the head space gas on a Hewlett Packard 5980 Series 2 gas chromatograph with Poropak-Q column and flame ionization detector ($CH_4$) or electron capture detector ($N_2O$). Dissolved concentrations of $CH_4$ and $N_2O$ were calculated from air–water Bunsen equilibrium coefficients (American Public Health Association 1992). Water for dissolved $O_2$ was collected directly into borosilicate glass syringes and reagents for a modified micro-Winkler technique (Wetzel and Likens 1991) were immediately added in the field.

### *Analysis of flow paths and hydrology*

We characterized paths of subsurface water flow both by direct measures of hydraulic heads (using sample wells as piezometers) and by following movements of in situ injections of a $Br^-$ conservative tracer (as NaBr; Hedin et al. 1990). Positions of piezometers were surveyed with a transit level in Field 1 and a level beam in Field 2. We determined water levels relative to a reference point (i.e., measures of hydraulic head) by lowering a graduated rod into piezometers and noting the change in electrical resistance of a circuit attached to this rod. The nested design of the network of piezometers in Field 1 allowed us to discern both horizontal and vertical components of subsurface water flow (Freeze and Cherry 1979). We evaluated distributions of hydraulic head throughout Field 1 on four occasions: August of 1993, and May, June, and July of 1994. We also measured hydraulic heads in Field 2 at 13 occasions during June–August of 1992, and sporadically in Field 3 and the eight additional single-well transects. Our quantitative analyses focus on Field 1, yet results from hydraulic-head distributions (all well fields and transects) and $Br^-$ tracer additions (Fields 1 and 2) did not differ greatly between the different soil–stream interfaces considered in this study (see *Results*).

We used $Br^-$ tracer additions for in situ estimates of subsurface water velocities and hydraulic conductivity. We added $Br^-$ to subsurface waters of Field 1 either as one-time pulse additions into sample wells, or as longer-term (<30 d) continuous additions from Mariotte bottles (Hedin et al. 1990) during carbon fertilizations (see below) into injection wells located between rows 2 and 3, or 3 and 4 (locations identified by triangles in Fig. 2A). To prevent any disturbance of natural paths of subsurface water flow we minimized volumes (<10 mL) of tracer pulses and minimized tracer delivery rates (<3 mL/min) from Mariotte bottles. Addition solutions were relatively concentrated (10 000 mg/L $Br^-$ for single injections; 1000 mg/L for continuous injections) to offset the strong and immediate dilution that occurred as small tracer volumes were introduced into rapidly moving (1–10 cm/h) subsurface waters. We labeled a larger volume of subsurface water by adding a single 3-L pulse of 100 mg/L $Br^-$-labeled water to well C4 in Field 2, thus creating a temporary (<8 h) influx of tracer-labeled water into subsurface water around this well. We subsequently monitored the distribution of $Br^-$ throughout Field 2 over 80 d.

We calculated subsurface water velocity by dividing the linear distance traveled by the peak in $Br^-$ concentration by the travel time of the pulse. We monitored $Br^-$ in a downflow well approximately every 10 min. We then calculated hydraulic conductivity ($K$, in meters per second) from Darcy's law as the product of subsurface water velocity ($v$, in meters per second) and effective porosity ($n$, dimensionless) divided by the observed gradient in hydraulic head along the flow path ($G = -\Delta h/\Delta l$ where $\Delta h$ is hydraulic head differential and $\Delta l$ is distance between two locations, both measured in meters) (Freeze and Cherry 1979, Harvey and Bencala 1993, Smith and Wheatcraft 1993):

$$K = (v \times n)/(-\Delta h/\Delta l). \quad (2)$$

We used total porosity as an approximate measure of effective porosity ($n$), by drying known volumes of saturated sediment collected with a 2.54-cm-diameter corer over 0–20 cm depth, and by dividing the volumetric water content by total sample volume (Freeze and Cherry 1979). Our analyses do not consider effects of anisotropy on $K$. We used daily average flow data from a U.S. Geological Survey gauging station located ~4 km downstream of Smith Creek to approximate hydrologic variations at our study sites.

### *Experimental carbon additions*

In August of 1993 we evaluated experimentally whether denitrification was limited by the supply of oxidizable DOC to near-stream environments. We used Mariotte bottles (Hedin et al. 1990) connected to injection wells (Fig. 3) to introduce dissolved carbon substrates known to be used by denitrifying bacteria (acetate, succinate, and propionate; each totalling 100 mg/L of C in the addition solution) into subsurface flow paths within the soil–stream interface. We injected the DOC solution once at each of three replicated locations in Field 1, indicated by triangles between rows 2 and 3 in Fig. 2A. Sample wells were located at two depths along the subsurface flow paths: (1) equal to the injection well (40 cm), and (2) more shallow (20 cm) to accommodate for upwelling of subsurface waters near the soil–stream interface (Fig. 3 and 2A). We included $Br^-$ (1000 mg/L) in the injection solution to: (1) confirm exact path(s) of subsurface flow between injection and sample wells, and (2) calculate the extent to which subsurface water was diluted by the injection solution. We minimized such dilution by keeping $Br^-$ and DOC concentrations high in the injection solution; this permitted <3 mL/min delivery rate of injection solution from each Mariotte bottle into the soil–stream interface. While we sampled six downwater wells (deep and shallow in each transect), our $Br^-$ tracer information showed that only four wells were affected (A2, B2, and C2 shallow, and B2 deep).

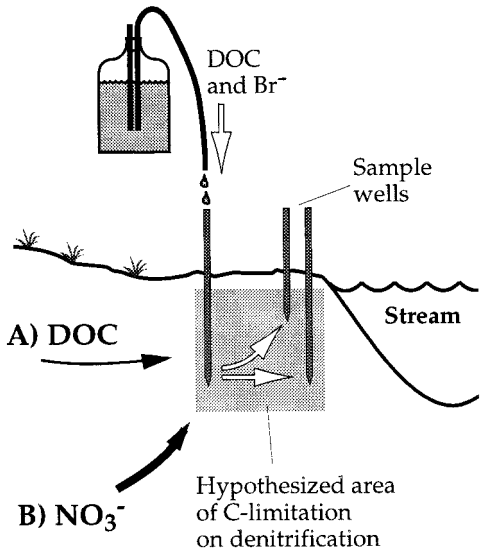


FIG. 3. Experimental introduction of oxidizable DOC (as acetate, succinate, and propionate) to subsurface waters within soil–stream interfaces at Smith Creek, Michigan, USA. The enrichment solution was added via a Mariotte bottle system that was connected to an injection well. $Br^-$ was included as a conservative tracer in the addition solution. Samples of subsurface waters were withdrawn from shallow (20 cm below soil surface) and deep (40 cm) wells located between the injection well and the stream. Closed arrows indicate dominant paths of natural supply of DOC (A) and $NO_3^-$ (B) via subsurface flow paths (Fig. 2B).

We collected water from sample wells (Fig. 3) to evaluate whether the experimental DOC addition affected concentrations of $NO_3^-$, $N_2O$, or $Cl^-$ in excess of what would be expected solely from dilution by the injection solution. Because background $Br^-$ levels were below our detection limit (<0.002 mg/L) we could calculate how much each sample was diluted by the injection solution as:

$$D = [Br^-]_{\text{sample well}}/[Br^-]_{\text{injection solution}} \quad (3)$$

where $D$ is the fraction of injection solution in the sample well, $[Br^-]_{\text{sample well}}$ is the measured concentration of $Br^-$ in the sample well, and $[Br^-]_{\text{injection solution}}$ is the concentration of $Br^-$ in the injection solution. The term $D$ allows us to predict how $NO_3^-$, $N_2O$, or $Cl^-$ were diluted by the presence of injection solution in each sample:

$$[X_{\text{predicted}}] = [X_{\text{background}}] \times (1 - D) \quad (4)$$

where $X$ is $NO_3^-$, $N_2O$, or $Cl^-$, $[X_{\text{predicted}}]$ is the predicted concentration of $X$ in the sample, and $[X_{\text{background}}]$ is the concentration of $X$ in the sample in absence of dilution by the injection solution. Throughout the experiment we estimated $[X_{\text{background}}]$ for each sample from second-order regressions of $[X]$ vs. time that were fitted using the pre- and post-experiment concentrations of $X$ in each sample well; regressions were all significant at $P < 0.1$ with $r^2$ values ranging from 0.45 to 0.97.

We examined the accuracy of this conservative tracer technique by evaluating whether Eq. 4 could accurately predict variations in $Cl^-$ that occurred over time in the different sample wells. We reasoned that $Cl^-$, since it is a biologically conservative element, would be affected solely by dilution and thus should be accurately predicted by Eq. 4. In all four sample wells, predicted variations in $Cl^-$ did not differ significantly ($P > 0.05$; $t$ test) from concentrations measured in sample wells (Fig. 12A and Table 3). We concluded that Eq. 4 was successful at predicting dilution effects due to the injection solution.

### *Stable isotopic analyses*

We analyzed N isotopes in Fields 1 and 2 during August 1992–November 1993. Samples were collected in acid-cleaned polyethylene bottles using the same syringe method as for dissolved nutrient sampling (described above). Samples were immediately preserved with mercuric chloride and frozen upon arrival at the laboratory (<3 h). Because subsurface waters could at times contain very low levels of $NO_3^-$ and/or $NH_4^+$ we needed relatively large sample volumes (up to 250 mL) to provide enough mass of N (>40 μmol) for isotopic analysis. We reasoned that 250 mL could not safely be withdrawn from a single well without modifying local subsurface flow, but instead chose to pool smaller sample volumes (<70 mL) from wells that were located at equal distances from the stream (i.e., located within the same row in Fig. 2A). This pooling approach was based on the consistently similar chemistry that occurred at equal distances from the stream (see *Results*); our N isotope information thus reflects volume-weighted trends along a transect perpendicular to the soil–stream interface.

We analyzed isotopic abundances of N on a VG Prism stable isotope mass spectrometer, modified to permit analysis of down to 40 μmol of N. Nitrate and $NH_4^+$ were extracted from water samples by a modified steam-distillation procedure (Bremner and Keeney 1966, Velinsky et al. 1989). Ammonia was distilled following adjustment of pH to >10, and collected by an HCl trap. The $NH_4^+$ was bound on a zeolite molecular sieve (Union Carbide Ionsiv W-85) and combusted to $N_2$ gas by a modified Dumas procedure (Macko 1981). Samples were oxidized at 850°C in evacuated ashed-quartz tubes with excess pre-combusted copper oxide and pure copper, cooled gradually overnight to prevent formation of carbon monoxide and nitrous oxides, and $N_2$ gas was separated cryogenically on a vacuum line for subsequent isotopic analysis. Nitrate was reduced to $NH_4^+$ by adding Devarda's alloy to the remaining sample and by shifting the pH to >10 with NaOH before a second distillation. The resulting $NH_4^+$ was treated as described above. Stable isotope ratios for N are expressed in per mil (‰) notation:

$$\delta^{15}N = [(R_{\text{sample}}/R_{\text{standard}}) - 1] \times 10^3$$

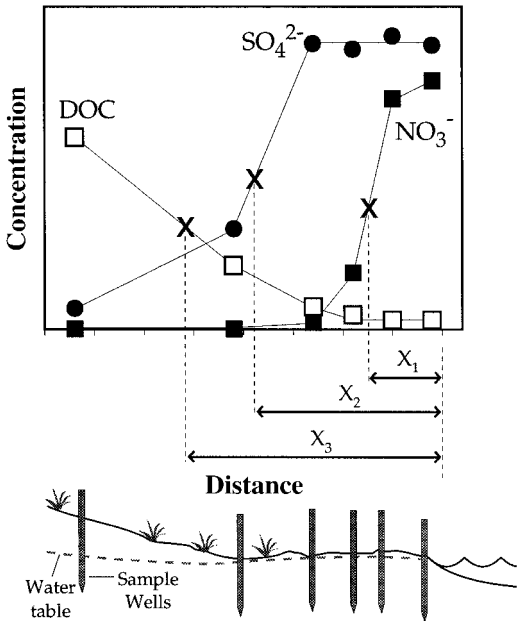


FIG. 4. Idealized example of statistical descriptions of concentration trends in $SO_4^{2-}$, $NO_3^-$, and DOC along the stream-to-inland transect. Lines indicate LOWESS fits to the concentration data. X identifies locations at which LOWESS-predicted concentrations are at the ''transition midpoint'' between maximum and minimum levels. $X_1$, $X_2$, and $X_3$ indicate distances of these 50% ''transition midpoints'' from the stream edge. In this example, the sequence of trends is $X_1 < X_2 < X_3$.

where $R$ is the abundance ratio of heavy to light isotope, and atmospheric $N_2$ gas is the standard (0‰). Analytical precision of replicate samples was <1‰.

### *Statistical analysis of thermodynamic predictions and spatial trends*

To evaluate whether variations in subsurface chemistry at our different sample sites followed our thermodynamic predictions (Fig. 1), we fit locally weighted robust regressions (LOWESS, tension = 0.5; see Wilkinson [1989]) to measured concentrations along the soil–stream interfaces. We determined the location of steep transitions in levels of electron donors or acceptors as where the LOWESS-predicted concentration was at the 50% midpoint between maximum and minimum levels (Fig. 4). These ''transition midpoints'' are operationally defined and represent our best approximation of the region of steep concentration change in a given electron donor or acceptor. In Fig. 4 we identify three such transition midpoints together with their distances from the stream edge along the interface ($X_1$ for $NO_3^-$, $X_2$ for $SO_4^{2-}$, and $X_3$ for DOC). This regression analysis permitted us to quantitatively test predictions of the sequence in which levels of electron donors and acceptors ought to change along the stream-to-inland gradient (right to left in Fig. 1). For example, our prediction (1)—that $NO_3^-$ ought to decrease before $SO_4^{2-}$—translates into the quantitative statement that $X_1$ should be consistently less than $X_2$ (Fig. 4) at all sites and all dates. We applied LOWESS regressions (Wilkinson 1989) to chemical data from all sample events at all soil–stream interfaces. We used a one-tailed $z$ test (Snedecor and Cochran 1989) to evaluate whether the observed sequence of LOWESS trends followed our theoretical predictions; each prediction of the type $X_1 < X_2$ was compared against the null model of equal probability (i.e., $P = 0.5$) of observing $X_1 < X_2$ vs. $X_1 > X_2$. In some cases the LOWESS fit failed to approximate a clear monotonic trend from high to low concentrations; we scored such trends as failing our prediction. However, a few periods of high discharge were associated with consistently high $SO_4^{2-}$ or low (<0.1 mg/L) $NO_3^-$-N across the soil–stream interface; these events were not scored as failing our predictions as long as they followed our thermodynamic expectations relative to other electron donors and acceptors. For example, consistently high $SO_4^{2-}$ together with a reduction in $NO_3^-$ along the soil–stream interface is consistent with our prediction (1), that $NO_3^-$ ought to decrease before $SO_4^{2-}$.

We used a split-plot ANOVA design to distinguish between spatial vs. temporal contributions to the observed variance of three principal solutes ($NO_3^-$, $SO_4^{2-}$, and DOC) in Field 2. Spatial variance was partitioned between contributions from the four different transects vs. from the six different rows, while temporal variance was estimated from 38 sample events over 2 yr (23 events for DOC). Analyses were performed on JMP IN 3.1.5 (Sall and Lehman 1996).

## RESULTS

### *Hydrologic flow paths*

In Fig. 2B we show a cross-sectional distribution of hydraulic heads and predicted paths of subsurface water flow in Field 1. We consistently found two dominant paths of subsurface flow: (1) Rapid vertical upwelling of deeper groundwater immediately near the stream channel (path A in Fig. 2B) with a vertical hydraulic gradient of approximately −2 to −3 mm/cm; and (2) weaker horizontal flow of shallow soil water parallel to the soil surface (path B in Fig. 2B), with an average horizontal hydraulic gradient of approximately −0.4 to −0.7 mm/cm. Our measures of hydraulic head were too infrequent to quantify short-term variations in flow paths (e.g., storage in stream banks during storm events; Freeze and Cherry 1979), yet comparisons between four sample events during May to August in Field 1 indicated that the relative strength of vertical vs. horizontal flow paths remained stable: the hydraulic gradient along path A was consistently between 2 to 3 times greater than the gradient along path B.

Injections of $Br^-$ tracer in Field 1 (locations identified by ▲ in Fig. 2A) also revealed strong vertical upwelling of subsurface water near (<1 m) the stream

edge at velocities of ~9 cm/h (along path A in Fig. 2B), together with weaker horizontal flow between wells at equal depth in the soil (path B in Fig. 2B). Based on a 30-d continuous injection of $Br^-$ at 40-cm depth in transect B (20 cm from stream edge; Fig. 2), we calculated that the injection well contributed only 5.5 ± 0.01% (mean ± 1 SE; $n = 12$ events) to the water in the equally deep well at location B2 (at stream edge), yet contributed 29 ± 0.03% ($n = 12$ events) to the water in the shallow (20 cm) well at the same B2 location. Additional $Br^-$ injections at 40-cm depth in transects A and C also resulted in $Br^-$ moving predominately to shallow rather than deep sample wells at locations A2 and C2. Additions of $Br^-$ tracer to wells in Field 2 showed that shallow (20-cm depth) subsurface water moved horizontally toward the stream at velocities ranging between ~0.4 and 0.9 cm/hr, and identified strong and more rapid upwelling in areas near the stream edge. Based on $Br^-$ tracer injections and measures of sediment porosity ($\bar{X}$ = 42%) we calculated the in situ hydraulic conductivity of the mixed inorganic–organic horizon as ~$6.9 \times 10^{-3}$ cm/s, a value that is representative for high-conductivity sand or gravel substrates (e.g., Smith and Wheatcraft 1993).

*Horizontal trends in subsurface water chemistry*

We found strong variations in the chemistry of subsurface waters within our different study sites in Smith Creek. For example, several nutrients ($NO_3^-$, $NH_4^+$, $SO_4^{2-}$, and DOC [dissolved organic carbon]) ranged more widely in concentrations within the 8-$m^2$ area of Field 1 than within stream waters of the entire 70-$km^2$ Augusta Creek drainage basin (14 sample sites over 1 yr; Hedin and Brown 1994). Our results revealed that these chemical variations were highly organized within each soil–stream interface, with steepest changes in concentrations occurring along our sampling transects in a direction perpendicular to the stream (specific sources of variation are examined in *Temporal vs. spatial variations . . .* , below). In Fig. 5 we show an example of how the chemistry of subsurface waters changed across our transects: electron acceptors ($O_2$, $NO_3^-$, $N_2O$, and $SO_4^{2-}$) were elevated in near-stream environments while electron donors ($NH_4^+$, DOC, and $CH_4$) were elevated in more inland environments. This spatial segregation of electron donors and acceptors was linked to different paths of subsurface flow (Fig. 2B): near-stream environments received inputs of deep and oxidized groundwater, while inland environments were primarily fed by shallow inputs of reduced soil water.

We used the stream-to-inland gradient in redox conditions to examine our thermodynamic predictions of how microbial metabolites ought to change as a function of decreasing p$\mathcal{E}$ (right to left in Fig. 1). The sequence of trends in Fig. 5 is typical for what we found at most sites and most sample dates, and is broadly consistent with our thermodynamic expectations (spe-

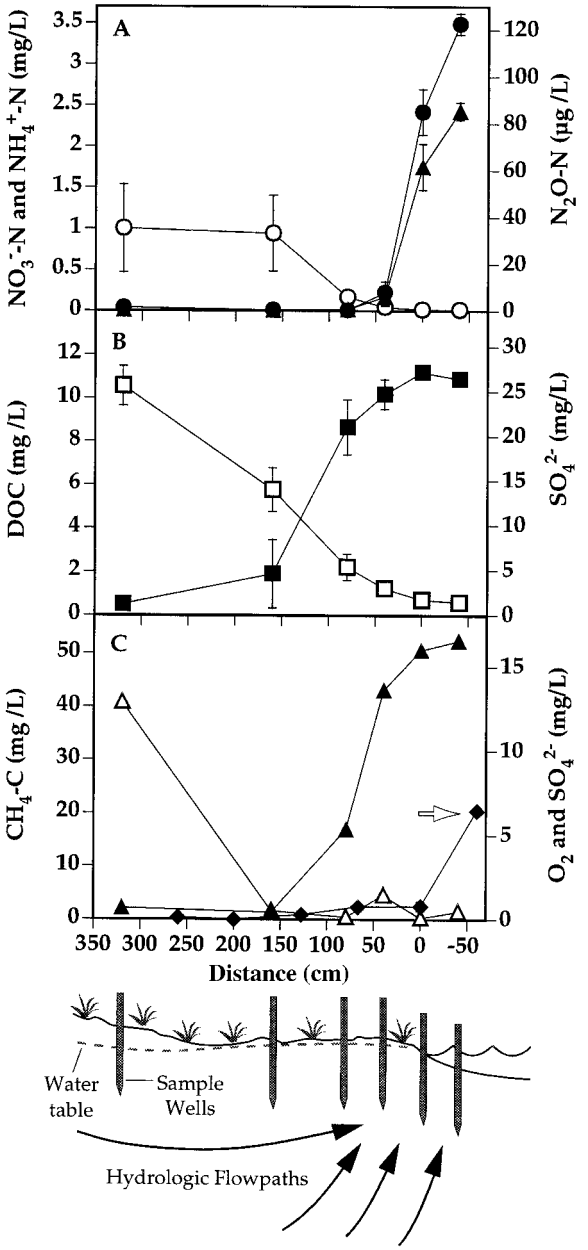


FIG. 5. Cross-sectional view of horizontal variations in subsurface water chemistry at 20-cm depth along soil–stream interfaces in Smith Creek, Michigan, USA. Solid symbols signify electron acceptors and open symbols signify electron donors. Values in (A) and (B) are averages of five parallel transects of Field 1 on 30 August 1993. (A) Inorganic forms of nitrogen: $NH_4^+$ (○), $NO_3^-$ (●), and dissolved $N_2O$ (▲). (B) DOC (□) and $SO_4^{2-}$ (■). (C) Trends in less frequently sampled constituents ($SO_4^{2-}$ included for comparison): dissolved $CH_4$ (△) and $SO_4^{2-}$ (▲) in Field 1 on 27 June 1994, and dissolved $O_2$ (◆) in two transects from Field 2 on 2 November 1992. The arrow points to a value for stream water concentrations of dissolved $O_2$. Error bars signify ±1 SE.

TABLE 2. Summary statistics for LOWESS fits to concentration trends in electron donors and acceptors along stream-to-inland transects in Field 1, Field 2, and all other fields. Data are the number of transects that were classified as consistent with each prediction, with the total number of transects in each category given in parentheses.

| Predicted sequence from stream to inland | Field 1 | Field 2 | Other fields† | All fields‡ |
|---|---|---|---|---|
| 1) $NO_3^- < SO_4^{2-}$ | 14 (14)*** | 38 (38)*** | 10 (14)* | 62 (66)*** |
| 2) $NO_3^- < NH_4^+$ | 10 (10)*** | 11 (13)*** | (0) | 21 (23)*** |
| 3) $NO_3^- <$ DOC | 12 (12)*** | 23 (23)*** | (0) | 35 (35)*** |
| 4) $N_2O < SO_4^{2-}$ | 6 (6)*** | 3 (3)*** | (0) | 9 (9)*** |
| 5) $N_2O <$ DOC | 6 (6)*** | 2 (2)*** | (0) | 8 (8)*** |
| 6) $SO_4^{2-} < CH_4$ | 2 (4) | 1 (1)§ | (0) | 3 (5) |
| Period sampled: | Jul. 1993–Oct. 1993 | Nov. 1991–Oct. 1993 | Feb. 1993–Jun. 1993 | NA‖ |

* $P < 0.05$, *** $P < 0.001$.
† All events from Field 3 plus 8 additional single transects.
‡ All events from all 11 soil–stream interfaces considered in this study.
§ Significance test not appropriate for single event.
‖ Not applicable.

cific predictions are evaluated below). Electron acceptors changed dramatically from near-stream to inland environments, following the sequence: reduction in $O_2$, followed by reduction in $NO_3^-$ and $N_2O$, followed by reduction in $SO_4^{2-}$ (Fig. 5A–C). Electron donors increased along the same gradient: accumulation in DOC, followed by accumulation in $NH_4^+$, followed by accumulation in $CH_4$ (Fig. 5A–C). Thus, forms of dissolved inorganic N changed steeply across the soil–stream interface so that oxidized forms (i.e., $NO_3^-$ and $N_2O$) were high in near-stream environments while the reduced form (i.e., $NH_4^+$) persisted in inland environments. Dissolved $N_2O$ contributed up to 7.2% of total dissolved inorganic N at our sites ($\bar{X} = 1.5\%$; $n = 167$ samples).

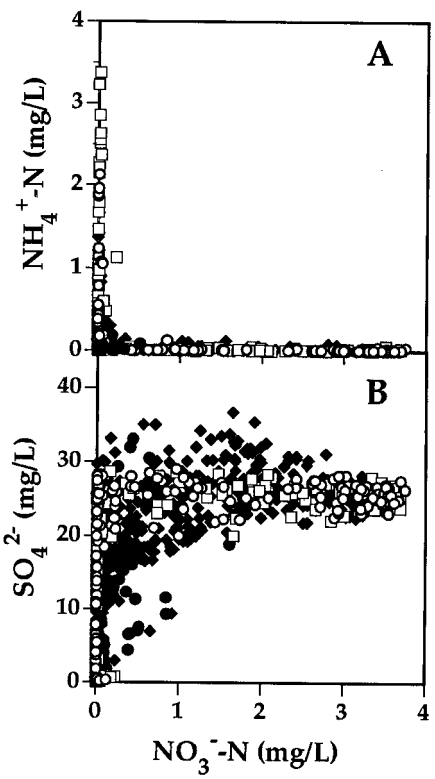


FIG. 6. Correlations between (A) $NH_4^+$ and $NO_3^-$ and (B) $SO_4^{2-}$ and $NO_3^-$ in soil–stream interfaces of Smith Creek, Michigan, USA, based on all (1400) individual samples of subsurface water from all study sites: Field 1 at 20-cm depth (○), 40-cm depth (□), Field 2 (♦), and all other fields (●).

In Table 2 we examine whether the trends in Fig. 5 were generally applicable to all study sites and all sample events. Specifically, we summarize whether the observed gradients in electron donors and acceptors (as described by LOWESS fits; Fig. 4) followed our different thermodynamic predictions. Our results show strong and consistent support for predictions 1 to 5, with observed sequences of trends differing significantly ($P < 0.05$; $Z$ test) from the null hypothesis of equal probability for the locations of trends in each different electron donor or acceptor. In fact, the observed trends failed to follow our predictions on only very few occasions: 4 of 62 transects did not support prediction 1, while 2 of 23 transects did not support prediction 2. However, for prediction 6 the sequence of observed trends did not differ significantly ($P > 0.05$; $Z$ test) from our null expectation.

We also analyzed for correlations between different electron donors and acceptors based on the >1400 individual samples of subsurface waters from all 11 sample areas and all 64 sample events. This analysis revealed several strong and predictable relationships (Figs. 6 and 7): First, we found a strict inverse relationship between $NH_4^+$-N and $NO_3^-$-N (Fig. 6A), with a virtual lack of any samples with $NH_4^+$ and $NO_3^-$ coexisting at levels >0.2 mg/L. Second, we found a highly predictable, yet more complex, relationship between $SO_4^{2-}$ and $NO_3^-$ (Fig. 6B). High levels of $NO_3^-$ occurred only in subsurface waters that already contained high (>20 mg/L) levels of $SO_4^{2-}$. Third, we found a strong and positive linear correlation ($r^2 = 0.88$; $P < 0.001$; $n = 167$) between $N_2O$ and $NO_3^-$ in subsurface waters from Fields 1 and 2 (Fig. 7A). This

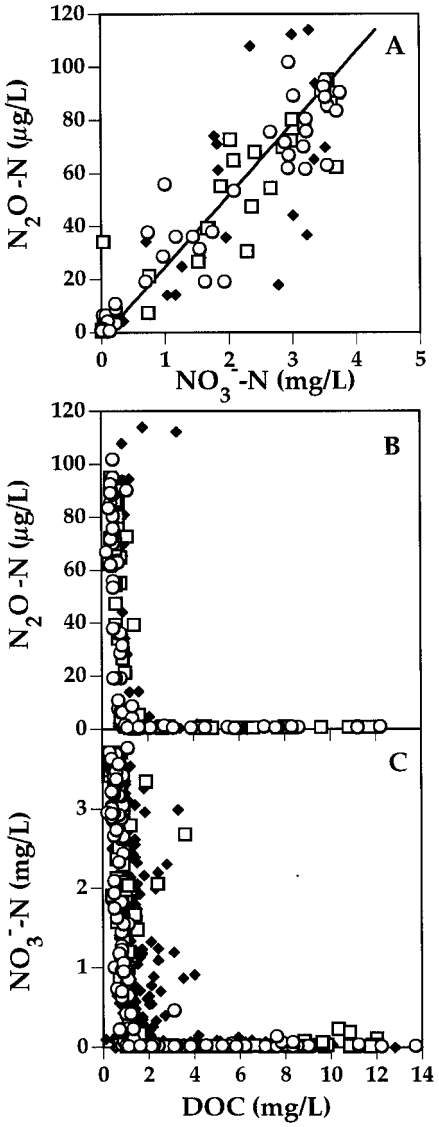


FIG. 7. Correlations between (A) $N_2O$ and $NO_3^-$, (B) $N_2O$ and DOC, and (C) $NO_3^-$ and DOC, in soil–stream interfaces of Smith Creek, Michigan, USA, based on individual samples of subsurface water: Field 1 at 20-cm depth (○), 40-cm depth (□), and Field 2 (♦). Line in (A) indicates statistically significant linear regression ($r^2 = 0.88$; $P < 0.05$).

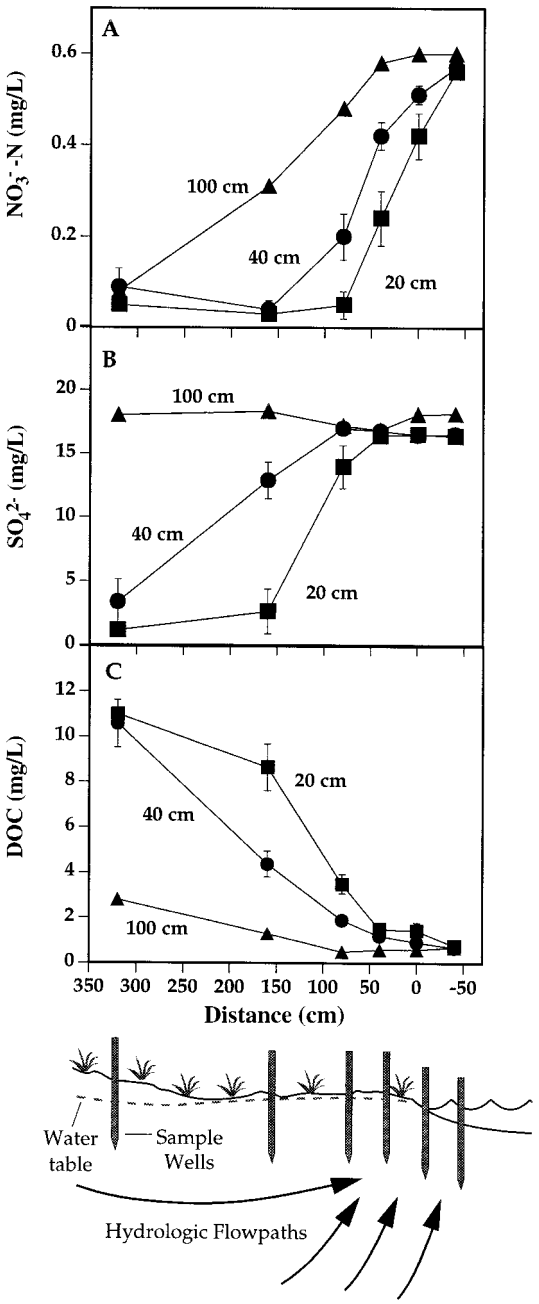


FIG. 8. Horizontal variations in subsurface water concentrations of (A) $NO_3^-$, (B) $SO_4^{2-}$, and (C) DOC as a function of depth below the soil surface in Field 1, Smith Creek, Michigan, USA. Subsurface waters were sampled on 8 June 1994, at 20-cm depth (■) ($n = 5$ transects), 40-cm depth (●) ($n = 5$ transects), and 100-cm depth (▲) ($n = 1$ transect). Error bars signify ±1 SE.

close link between $N_2O$ and $NO_3^-$ was also apparent in our analyses of solute trends across soil–stream interfaces, with high levels of both $N_2O$ and $NO_3^-$ in near-stream environments (Fig. 5A). Fourth, we found strong and inverse relationships between oxidized forms of N (i.e., $NO_3^-$ and $N_2O$) and DOC (Fig. 7B and C). Closer examination of these relationships revealed that $N_2O$ and $NO_3^-$ only accumulated or persisted in subsurface waters that contained low levels of DOC (<2 mg/L). Conversely, subsurface waters with DOC at levels >4 mg/L never showed any accumulation of $N_2O$–N above 0.6 μg/L, or of $NO_3^-$-N above 0.3 mg/L.

### *Vertical trends in subsurface water chemistry*

While our information is limited to $NO_3^-$, $SO_4^{2-}$, and DOC in Field 1, our results show that the chemistry of subsurface waters also varied strongly with depth of soils or sediments (Fig. 8). These vertical variations

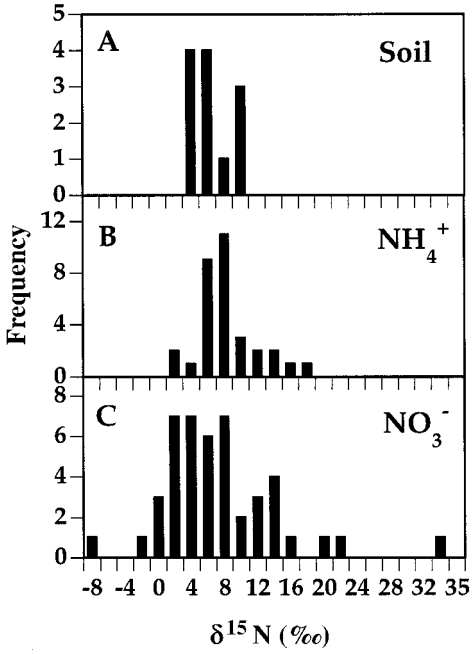


FIG. 9. Frequency distributions of $\delta^{15}N$ natural isotopic values for (A) total soil N in upper 40 cm of soils, (B) $NH_4^+$ in subsurface waters, and (C) $NO_3^-$ in subsurface waters in Fields 1 and 2, Smith Creek, Michigan, USA.

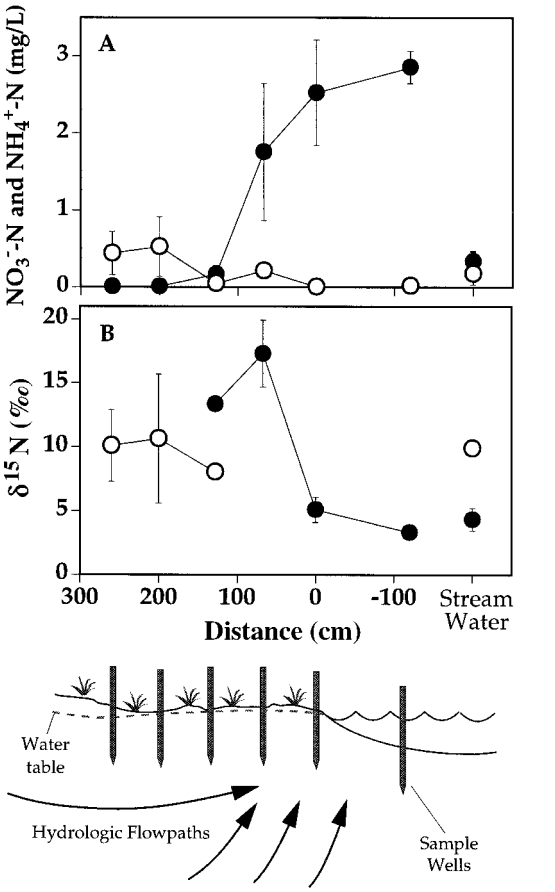


FIG. 10. (A) Variations in concentrations and (B) $\delta^{15}N$ natural isotopic abundances of $NH_4^+$ (○) and $NO_3^-$ (●) in subsurface waters at 20-cm depth in Field 1 and in stream water of Smith Creek, Michigan, USA. Values are means from three different sample events during July–November 1993. Error bars signify ±1 SE ($n$ = 3 samples). Missing values signify lack of adequate mass of N (i.e., <40 μmol) for isotopic analysis.

were manifested as a gradual weakening in the strength of the horizontal concentration trend of each solute as a function of depth. For example, the decline in $SO_4^{2-}$ between near-stream and inland environments was steep at 20-cm depth, weaker at 40-cm depth, and was completely lost at 100-cm depth (Fig. 8B). In contrast to $SO_4^{2-}$, the horizontal trends in $NO_3^-$ and DOC changed more gradually as a function of depth (Fig. 8A and C).

### *Trends in $\delta^{15}N$ isotope abundances*

The $\delta^{15}N$ isotopic values of total soil N (0–45 cm depth) ranged between 4.1 and 9.9‰ ($n$ = 13; Fig. 9A) within Fields 1 and 2. While average $\delta^{15}N$ values for subsurface $NH_4^+$ (8.2‰; $n$ = 32; 13 transects) and $NO_3^-$ (7.3‰; $n$ = 45; 13 transects) were within the range measured for total soil N, individual $\delta^{15}N$ measures were substantially outside this range (Fig. 9B and C). For example, 12 out of 45 $\delta^{15}N$ values for $NO_3^-$ were elevated above 10‰ (maximum: 34.1‰) while 3 values were depleted below 0‰. Similarly, 6 out of 32 $\delta^{15}N$ values for $NH_4^+$ were elevated above 10‰.

Closer inspection revealed fine-grained spatial variations in $\delta^{15}N$ isotopic abundances of $NO_3^-$ across soil–stream interfaces. The most strongly enriched values of $\delta^{15}N$–$NO_3^-$ occurred immediately inland of the peak in $NO_3^-$ concentrations on 10 out of 13 sample dates, corresponded with the location of the $NO_3^-$ peak on an additional 2 dates, and occurred between the stream and the $NO_3^-$ peak on only 1 single date. This pattern of elevated $\delta^{15}N$–$NO_3^-$ immediately inland of the $NO_3^-$ peak is illustrated graphically in Fig. 10, in which we summarize three consecutive sample events during a period of stable chemistry from July to November. In contrast to $NO_3^-$, we could not find any systematic spatial or seasonal pattern to the observed variations in $\delta^{15}N$ of $NH_4^+$. The lack of $\delta^{15}N$ values for $NO_3^-$ at distances >120 cm and for $NH_4^+$ at distances <120 cm in Fig. 10 are due to N levels less than the 40 μmol required for isotopic analysis.

### *Temporal vs. spatial variations in subsurface chemistry*

While electron donors and acceptors showed strong and predictable trends within soil–stream interfaces of Smith Creek, the exact location and magnitude of these patterns varied over time. A split-plot nested ANOVA analysis of $NO_3^-$ concentrations in Field 2, for which we have the longest continuous chemical record (38

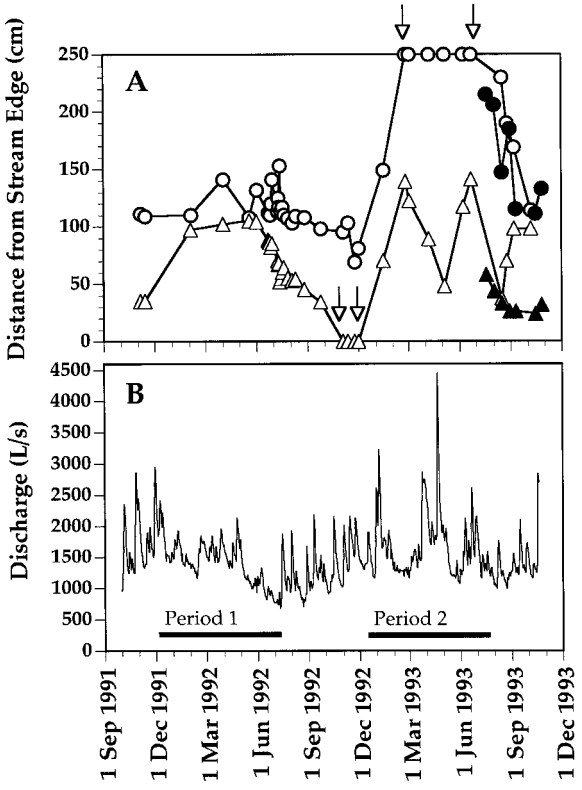


FIG. 11. Temporal variation in redox gradient. (A) Variations in location of ''transition midpoints'' (as described by LOWESS regressions; Fig. 4) for gradients in $SO_4^{2-}$ (circles) and $NO_3^-$ (triangles) during October 1991–October 1993 in Field 1 (open symbols) and during late 1993 in Field 2 (closed symbols). (B) Discharge during October 1991–October 1993 at the USGS gauging station located on Augusta Creek, Michigan, USA. Bars identify periods of similar variations in temperature but distinctly different variations in hydrology: low variability (period 1) vs. high variability (period 2).

events during November 1991–October 1993), showed that 26% of total variance ($P < 0.001$; df = 5) was explained solely by horizontal trends along sampling transects (i.e., between-row variability) as displayed in Fig. 5. Only 0.5% of total variance ($P > 0.71$; df = 3) was explained by between-transect variability, indicating that horizontal trends generally were very similar among replicate transects. Temporal variations alone (between sample events) could explain 11% of total variance ($P < 0.001$; df = 36). The interaction effect between transects and time explained an additional 23% of total variance ($P < 0.001$; df = 180), indicating that the location and shape of horizontal trends along transects changed significantly over time. Results for $SO_4^{2-}$ and DOC were qualitatively similar to those of $NO_3^-$.

Our analyses of locations of the ''transition midpoint'' for gradients of $NO_3^-$ and $SO_4^{2-}$ along the soil–stream interface (Fig. 11A) revealed extended periods during which the location of both gradients changed little (e.g., January–June of 1992 for $SO_4^{2-}$), periods of gradual change in locations of gradients (e.g., June–November of 1992 for $NO_3^-$), and shorter periods of rapid change in the location of one or both of the gradients (e.g., December 1992–March 1993). The $NO_3^-$ gradient appeared to have a seasonal component, with the ''transition midpoint'' moving closer to the stream during fall and early winter, and remaining inland during late winter and spring (Fig. 11A). To explore whether these temporal variations in location of redox gradients might be linked to hydrologic variations, we contrasted two equally long periods (January–July) with similar temperature conditions but markedly different hydrologic variability (Fig. 11B). Period 1 (low variability) had only 3 days with discharge exceeding the 90th percentile for daily discharge rates over the 2-yr period of this study. Period 2 (high variability) had 40 days that exceeded the 90th percentile discharge rate. Trends in $NO_3^-$ and $SO_4^{2-}$ were well developed and more stable (particularly for $SO_4^{2-}$) during the hydrologically less variable period 1 (Fig. 11A). In contrast, we found a complete loss of the $SO_4^{2-}$ gradient (identified by open arrows in Fig. 11) and enhanced temporal variations in the $NO_3^-$ gradient during the hydrologically more variable period 2.

### *Experimental carbon fertilization*

For all experimental DOC additions, we found no significant differences ($P > 0.05$; *t* test) between observed concentrations in $Cl^-$ vs. concentrations predicted to occur solely from dilution by the injection solution (Table 3). For example, in Fig. 12A we show the close correspondence ($P > 0.05$; *t* test; $n = 13$ sample events) between predicted and observed $Cl^-$ that persisted throughout the 30-d DOC addition at location B2. In contrast, we found that DOC additions caused strong reductions of $NO_3^-$ in subsurface waters, to levels that were significantly (27–81%; $P < 0.05$; *t* test) below those predicted solely on the basis of dilution (Table 3). In Fig. 12B we show that $NO_3^-$ declined immediately following DOC enrichment at location B2, and that throughout the experiment $NO_3^-$-N was reduced by 80% from the expected mean level of 1.5 mg/L (1 SE = 0.08; $n = 13$) to the observed mean of 0.28 mg/L (1 SE = 0.04; $n = 13$). However, the response in $NO_3^-$ was not always so immediate. Reduction in $NO_3^-$ at site C2 increased gradually from 0% on day 1 to 52% on the final day of the experiment (day 11), and averaged 31% throughout the experiment ($P < 0.05$; *t* test; $n = 7$; Table 3). In contrast, we found no statistically significant ($P > 0.05$; *t* test; $n = 12$) $NO_3^-$ reduction in response to 22 d of DOC addition at location A2.

The experimental DOC additions also caused strong declines (41–77%) in dissolved $N_2O$ in three out of four sample wells (Table 3). We cannot, however, assign statistical significance to these reductions since we sampled for $N_2O$ only on three occasions (before, during, and after the experiment) and our design was

TABLE 3. Summary statistics for experimental dissolved organic carbon (DOC) additions to sites A2, B2, and C2 in Field 1 at Smith Creek, Michigan, USA. Predicted concentrations are based on Eq. 4, assuming that concentrations are affected solely by dilution from the injection solution. Observed concentrations are average concentrations measured during each experiment. Data are means ± 1 SE.

| Downwater sampling well | $N$† | $Cl^-$ (mg/L) | | $NO_3^-$–N (mg/L) | | $NO_3^-$ Loss (%)‡ | $N_2O$–N§ (μg/L) | | $N_2O$ loss (%)‡ |
|---|---|---|---|---|---|---|---|---|---|
| | | Predicted | Observed | Predicted | Observed | | Predicted | Observed | |
| A2, shallow | 12 | 4.0 ± 0.12 | $4.0^{NS}$ ± 0.10 | 3.3 ± 0.09 | $3.1^{NS}$ ± $0.17^{NS}$ | 6.1 | 50 | 55 | −10 |
| B2, shallow | 13 | 3.2 ± 0.16 | $3.1^{NS}$ ± 0.12 | 1.5 ± 0.08 | 0.28*** ± 0.04 | 81 | 44 | 10 | 77 |
| B2, deep | 13 | 4.2 ± 0.09 | $4.1^{NS}$ ± 0.10 | 2.8 ± 0.04 | 2.0*** ± 0.18 | 27 | 78 | 46 | 41 |
| C2, shallow | 7 | 3.0 ± 0.26 | $2.9^{NS}$ ± 0.17 | 1.6 ± 0.14 | 1.1* ± 0.16 | 31 | 45 | 18 | 60 |

* $P < 0.05$, *** $P < 0.001$, $^{NS}$ not significant at $P < 0.05$.
† $N$ = number of sample events for both $Cl^-$ and $NO_3^-$.
‡ Percentage loss refers to the entire experimental period.
§ $N_2O$ was only sampled once during the experimental additions.

therefore not adequately replicated. The measured reductions were nevertheless large, as exemplified by reduction in $N_2O$–N from the expected level of 44 to 10 μg/L in the 20-cm-deep well at site B2. We interpret the return of dissolved $N_2O$ to approximately pre-experiment levels once the DOC addition was ended as further evidence that, despite lack of adequate statistical evidence, DOC had a real effect on $N_2O$.

## DISCUSSION

Our study of Smith Creek supports the idea that narrow regions of terrestrial–aquatic interfaces can serve as focal points for nutrient transformations within landscapes. Our results indicate that the biogeochemical significance of such regions is caused by the intersection of two steep gradients: (1) a thermodynamic gradient between oxidized near-stream environments and reduced inland environments, and (2) a hydrologic gradient between rapid upwelling of deeper water in areas near the stream and less rapid transport of shallow soil water from inland environments toward the stream. This intersection appears to be central to understanding how soil–stream interfaces function within landscapes since it defines regions where high potential for biogeochemical activity (due to close proximity of electron donors and acceptors) coincides with rapid transport of subsurface water from terrestrial to aquatic ecosystems. It is at or near this intersection that we found evidence for important N transformations, including an exceptionally strong potential for denitrification.

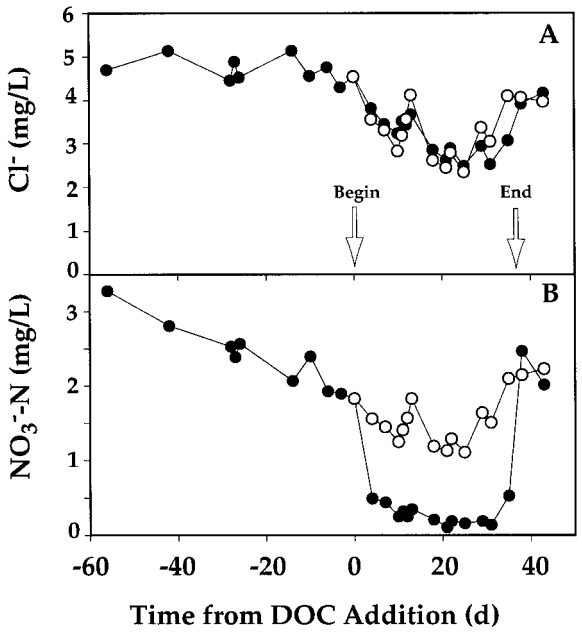


FIG. 12. Concentrations of (A) $Cl^-$ and (B) $NO_3^-$ in response to experimental introduction of oxidizable DOC (as acetate, succinate, and propionate) to subsurface waters at site B2 in Field 1 at Smith Creek, Michigan, USA. ● = concentrations measured in subsurface waters; ○ = concentrations predicted based solely on dilution by the injection solution. Arrows indicate beginning and end of the experiment.

The observation that soil–stream interfaces are biogeochemically highly variable environments is by no means new (e.g., Hill 1990, Dahm et al. 1991, Hendricks and White 1991, McDowell et al. 1992, Jones et al. 1995*a*, Groffman et al. 1996, Hill 1996, Jones and Holmes 1996), yet the factors that control this variability have remained elusive. Our results from Smith Creek illustrate that this variability can be a predictable outcome of the interaction between thermodynamic constraints on microbial communities and supplies of electron donors and acceptors via subsurface flow paths. Our results show that a thermodynamic perspective can enhance our understanding of mechanisms of nutrient transformations, and can thus improve our ability to predict how soil–stream interfaces function as biogeochemical systems. We propose that in many landscapes the sustained ability of soil–stream interfaces to remove $NO_3^-$ by denitrification ought to be controlled by the supply of oxidizable dissolved organic carbon (DOC) (as electron donor) to narrow regions at the soil–stream interface.

### *Thermodynamic controls on biogeochemical patterns and microbial processes*

The most general conclusion of this study is that a thermodynamic approach can aid our understanding of

how soil–stream interfaces function as biogeochemical systems. Despite strong spatial and temporal variability, we found that distributions of electron donors and acceptors remained organized in a highly predictable thermodynamic sequence with distance from the stream and with depth of soils/sediments (Figs. 5 and 8 and Table 2). From this we conclude that contributions of different microbial transformations followed our predictions in Fig. 1 from near-stream to inland environments: aerobic respiration, denitrification, nitrification, sulfate reduction, and methanogenesis. The biogeochemical consequences of such thermodynamic sequences have been studied in lake or marine sediments (Stumm and Morgan 1981, Howarth 1993) and in groundwaters (Chapelle and Lovely 1992), yet their role in controlling element transformations within soil–stream interfaces remains largely unexplored.

The lack of clear support for prediction 6—that $SO_4^{2-}$ concentrations ought to decrease before $CH_4$ increases—may reflect insufficient precision of the LOWESS technique to evaluate this prediction, particularly since both $SO_4^{2-}$ and $CH_4$ are expected to change in close proximity to each other (Fig. 1). In addition, the presence of microenvironments of differing redox state (e.g., inside vs. outside soil particles) has been found to promote the cooccurance of sulfate reduction and methanogenesis (Howarth 1993). Yet despite this lack of statistical significance, all five transects that we evaluated showed strong decreases in $SO_4^{2-}$ and strong increases in $CH_4$ along the stream-to-inland gradient—a pattern that qualitatively follows prediction 6 and Fig. 1.

Correlation analysis based on all individual samples from all soil–stream interfaces provided further evidence that thermodynamic constraints were a primary determinant for patterns of variation in subsurface water chemistry. Because $NH_4^+$ and $NO_3^-$ do not coexist at significant levels in environments that are at or near thermodynamic equilibrium (Fig. 1), we interpret the mutually exclusive relationship between $NH_4^+$ and $NO_3^-$ (Fig. 6A) as supporting the idea that redox gradients provided the dominant control on forms of inorganic nitrogen within soil–stream interfaces of Smith Creek (cf. similar patterns described in McDowell et al. [1992] and McClain [1994]). The area of active nitrification, where $NH_4^+$ and $NO_3^-$ coexist out of equilibrium, must therefore be limited to a zone that is spatially so narrow that it is rarely sampled, and/or nitrification must be rapid enough for the conversion from $NH_4^+$ to $NO_3^-$ to nearly always be complete. In both cases, individual samples of subsurface water would be dominated either by $NH_4^+$ or $NO_3^-$ depending on whether or not $O_2$ is present as an electron acceptor to permit nitrification.

Our results do not support the contention that $NH_4^+$ gradients across riparian zones are steeper in tropical than in temperate-zone forested or agricultural landscapes (McDowell et al. 1992). In fact, we found a greater range in $NH_4^+$-N concentrations (0–3.4 mg/L; Fig 6A) over a smaller distance ($<$3.5 m) than reported for Puerto Rican tropical forests (McDowell et al. 1992). Rather than varying according to ecosystem type or climate, we expect the strength of gradients across soil–stream interfaces to result from interactions of several local factors that control sources and sinks of $NH_4^+$ and $NO_3^-$: external hydrologic inputs of inorganic N, pool sizes of mineralizable N, C:N ratios of local soil organic matter, nitrification rates, losses by denitrification, net demands by riparian vegetation or microbial communities, and hydrologic dilution by the mixing of different subsurface flow paths with differing chemistry. While $NO_3^-$ enters our soil–stream interfaces via upwelling of $NO_3^-$-rich groundwater (Figs. 2, 5, and 8), we cannot unequivocally trace the source for $NH_4^+$. Yet, the low C:N ratio ($\sim$14) of soil organic matter, and the similarity of $^{15}N$ signatures of total soil N and dissolved $NH_4^+$ (Fig. 9), suggest mineralization as an important source for $NH_4^+$.

The more complex statistical relationship between $NO_3^-$ and $SO_4^{2-}$ (Fig. 6B) is consistent with the preferential use of $NO_3^-$ over $SO_4^{2-}$ as electron acceptor during microbial metabolism (our prediction 1) in that significant reduction in $SO_4^{2-}$ did not occur unless $NO_3^-$-N was first reduced to less than $\sim$0.2 mg/L. As a result, $NO_3^-$-N varied strongly in subsurface waters (range: 0–3.8 mg/L) while $SO_4^{2-}$ typically remained near groundwater levels (range: $\sim$20–30 mg/L), except for inland environments in which $NO_3^-$ had first been strongly depleted.

Moreover, our correlation analyses pointed to a link between the N cycle and supplies of electron donors in the form of DOC. Dissolved $N_2O$ and $NO_3^-$ showed very similar spatial and temporal variations within the soil–stream interfaces (Fig. 7A). Perhaps more striking were the strong and inverse relationships that existed between these oxidized forms of N ($NO_3^-$ and $N_2O$) and DOC (Fig. 7B and C), suggesting that oxidized N forms only accumulated in environments with low supplies of DOC. The biogeochemical implications of this apparent link between DOC and dissolved forms of N are further explored in *Carbon control on denitrification,* below.

### *Transformations of N*

Our measures of N chemistry point to the near-stream area as a potentially important ''control-point'' for N transformations. First, the strong accumulation of $N_2O$ within $<$40 cm of the soil–stream boundary indicates the presence of denitrification, nitrification, or a combination of both processes in this region (Firestone and Davidson 1989). Second, the steep gradients in $NH_4^+$ and $NO_3^-$ immediately inland of the soil–stream boundary point to the immediate near-stream region as a thermodynamically favorable area for N transformations. Trends in $NO_3^-$-N were particularly steep and could range from $>$3 mg/L to below our detection limit over distances of $<$1 m.

In the absence of strong isotopic differences between sources, natural $\delta^{15}N$ abundances can be used to understand mechanisms, location, and kinetics of dominant N transformations (Macko and Ostrom 1994, Nadelhoffer and Fry 1994). Microbial denitrification is associated with strong isotopic fractionation (about +30‰; Blackmer and Bremner 1977, Vogel et al. 1981, Nadelhoffer and Fry 1994) that causes any $NO_3^-$ that remains in the local environment to be progressively enriched in isotopically heavier $^{15}N$. In contrast, microbial nitrification causes remaining $NH_4^+$ to become progressively enriched in $^{15}N$, while the product ($NO_3^-$) becomes isotopically lighter (Macko and Ostrom 1994, Nadelhoffer and Fry 1994). Transformations of N by denitrification vs. nitrification are therefore associated with distinctly different shifts in $\delta^{15}N$ signatures of the $NH_4^+$ or $NO_3^-$ that remains in local environments.

Our data on $\delta^{15}N$ isotope abundances show that significant denitrification occurred within a well-defined zone immediately inland of the soil–stream boundary. Values of $\delta^{15}N$–$NO_3^-$ were strongly elevated (up to +34‰) in the region of the soil–stream interface that coincided with the steepest gradient in $NO_3^-$ (Fig. 10) and with an accumulation of dissolved $N_2O$, which is an intermediate metabolite in denitrification. Such a fractionation is too large to stem from variations in N source, or from any N transformation other than denitrification. Based on a value of +5‰ for groundwater $NO_3^-$ (Figs. 9 and 10B) and an instantaneous fractionation factor ($\alpha$) of +30‰ for denitrification (Blackmer and Bremner 1977, Vogel et al. 1981), we calculate that the observed natural abundances of between +15 to +34‰ (Figs. 9 and 10B) were associated with losses of up to 30–60% of original $NO_3^-$ by the mechanism of denitrification. We conclude that denitrification was rapid enough, relative to hydrologic supply of $NO_3^-$, to significantly deplete $NO_3^-$ within this region of the soil–stream interface. In contrast, $\delta^{15}N$–$NO_3^-$ was typically not elevated in the high-$NO_3^-$ waters immediately at or near the stream (Fig. 10B), indicating that hydrologic $NO_3^-$ transport dominated over denitrification losses in this region due to ''short-circuiting'' of riparian N retention.

We did not find evidence for highly localized effects of nitrification on natural $\delta^{15}N$ abundances. The interface between dominance of $NH_4^+$ vs. $NO_3^-$ was never characterized by enriched values in $\delta^{15}N$–$NH_4^+$ together with depleted $\delta^{15}N$ of $NO_3^-$, as would be expected if the observed trends in N chemistry were controlled solely by nitrification. We therefore conclude that nitrification was either less localized or generally less important than denitrification in defining N transformations within our soil–stream interfaces.

### *Carbon control on denitrification*

We interpret the observation that $NO_3^-$ and $N_2O$ only accumulated in waters with low DOC as support for the hypothesis that denitrification of $NO_3^-$ and $N_2O$ to dinitrogen gas ($N_2$) was primarily limited by carbon supply (i.e., electron donor limitation) to near-stream environments in Smith Creek. Studies of high-$NO_3^-$ groundwater systems have similarly suggested that denitrification can be limited by carbon supply (e.g., Bradley et al. 1992, Starr and Gillham 1993). In addition to our indirect evidence, we found direct experimental support for this hypothesis in that our additions of oxidizable forms of carbon (acetate, propionate, and succinate) to near-stream environments caused substantial reductions in $NO_3^-$ and $N_2O$ in three out of four sample wells. Differences between wells in the timing and extent of response to DOC enrichment may have resulted from local-scale variations in chemical environments (e.g., p$\mathcal{E}$) or in size or activity of populations of denitrifying bacteria.

Experimental DOC additions induced remarkable increases in $NO_3^-$ removal within soil–stream interfaces at Smith Creek. Based on in situ measures of hydraulic conductivity ($6.9 \times 10^{-3}$ cm/s), hydraulic gradients (ca. −0.25 cm/cm), and the measured reduction in $NO_3^-$ due to DOC addition (Fig. 12B), we calculate that removal of $NO_3^-$-N increased by as much as 1.8 $g \cdot m^{-2} \cdot d^{-1}$. This rate is equivalent to 6600 $kg \cdot ha^{-1} \cdot yr^{-1}$ when expressed on a per hectare basis (note that this rate only applies to the biogeochemically active sediments in the riparian zone), which is two orders of magnitude greater than other values expressed as kilograms per hectare per year of biogeochemically active ''riparian zone'' (10–39 $kg \cdot ha^{-1} \cdot yr^{-1}$; Lowrance et al. 1995). We conclude that with adequate supplies of oxidizable carbon to the right location, near-stream areas can possess a remarkable potential for $NO_3^-$ removal from subsurface waters. In fact, removal rates were rapid enough in the transect-B experiment to change $NO_3^-$-N concentrations from 1.5 mg/L to as low as a few tenths of a milligram per liter over as little as 20 cm of flow path.

### *Link between hydrology and thermodynamics*

Our results suggest that the biogeochemical function of soil–stream interfaces at Smith Creek resulted, to a great degree, from the interaction between thermodynamic constraints on microbial metabolism and different hydrologic flow paths. Energy-rich electron donors (DOC, $CH_4$, and $NH_4^+$) were delivered to the near-stream area via shallow flow paths (path B in Fig. 2B) that originated in close proximity to organic-rich horizons in inland soils. In contrast, electron acceptors were delivered via oxidized groundwater that was rich in $NO_3^-$ and $SO_4^{2-}$ (e.g., path A in Fig. 2B). It is this confluence of electron donors and acceptors that creates the biogeochemical potential of these soil–stream interfaces; microbial communities respond by using the resulting redox gradient to derive energy for growth. Our results suggest that the redox gradient was only moderately sensitive to hydrologic or seasonal varia-

tions since, throughout 2 yr in Field 2, it only completely disappeared during a brief winter period and was weakened during a period of unusually high hydrologic variability (Fig. 11).

### *General function of soil–stream interfaces*

It is difficult to generalize from this study since we considered a limited number of locations along a single stream. Nevertheless, our basic thermodynamic and hydrologic approach is likely to aid in the identification of mechanisms that maintain the biogeochemical structure and function of soil–stream interfaces at other locations, too.

For Smith Creek, we found that denitrification did not consume all $NO_3^-$ that reached the soil–stream interface (cf. Figs. 5 and 12). Thus, our study sites provide an example of riparian habitats that can influence, but not fully control, fluxes of inorganic N across the terrestrial–aquatic interface. We propose that the effectiveness of denitrification as a mechanism for N retention depends critically on whether microbial denitrification reactions are thermodynamically favored in riparian environments with rapid throughput of terrestrially derived water. Such hydrologically active regions function within landscapes as conduits that connect watershed processes and the chemistry of surface waters. We propose that the sustained ability of soil–stream interfaces to remove $NO_3^-$ via denitrification is likely to depend on three dominant factors: (1) the spatial location of ''conduit'' areas with high hydrologic throughput, (2) whether the local redox environment promotes rapid denitrification in these hydrologically active areas, and (3) the rate of supply of oxidizable carbon from inland environments to these hydrologically active areas. Other studies have proposed that a similar redox interface may occur at the interface between uphill soils and the beginning of the riparian zone (e.g., Jacobs and Gilliam 1985*b*, Lowrance 1992); the effectiveness of denitrification at this interface ought to follow the same general factors as we propose for the soil–stream interface.

We expect the type of limitation on denitrification to change as a function of the ratio between supplies of oxidizable DOC vs. $NO_3^-$, with carbon limiting at low ratios and $NO_3^-$ limiting at high ratios of DOC to $NO_3^-$. This means that it can be difficult to unequivocally determine whether DOC or $NO_3^-$ limits denitrification in areas with steep redox gradients, such as across soil–stream interfaces. While $NO_3^-$ removal by denitrification can be carbon limited in near-stream environments, as we found in this study, denitrification is likely to be simultaneously limited by $NO_3^-$ in the more DOC-rich inland environments of soil–stream transects. Yet our study suggests that DOC limitation should be of greatest applied significance for understanding the ability of soil–stream interfaces to remove $NO_3^-$ via denitrification. That is, regions with high hydrologic throughput of $NO_3^-$ will by thermodynamic necessity be rich in electron acceptors, and therefore most likely limited by DOC.

It should be possible to predict how different soil–stream interfaces function within landscapes solely based on relatively straightforward thermodynamic and hydrologic analyses. Hydrologically active areas that are in close proximity to environments that export electron donors (e.g., wetlands or organic histosols) probably possess the strongest ability to buffer dissolved N losses from agricultural or other sources. However, the idea of actively managing N losses from soil–stream interfaces by directly supplying oxidizable DOC may be difficult and associated with negative effects on downstream ecosystems. Enhancement of DOC delivery via passive management, such as the promotion of wetlands and/or organic-rich soils, may be a more reasonable approach.

## Acknowledgments

We thank Michael Klug and Richard Losee for advice and assistance in the field, Norman Granneman and Paul Klimek of the USGS for assistance with discharge data from Augusta Creek. We thank Clifford Dahm, Peter Groffman, Gene Likens, Jason Neff, Bill Sobzack, Peter Vitousek, Nancy Grimm, and two anonymous reviewers for comments on the text, Chuck McCulloch and Naiomi Altman for statistical advice. This work was supported by grants from the National Science Foundation (BSR92-08395, to L. O. Hedin, N. E. Ostrom, and G. P. Robertson) and the A. W. Mellon Foundation (to L. O. Hedin), and is contribution number 794 to the W. K. Kellogg Biological Station of Michigan State University.

## Literature Cited

Alpkem. 1992*a*. Ammonia in seawater. Document Number 000674. Alpkem, Wilsonville, Oregon, USA.

———. 1992*b*. Silica in seawater. Document Number 000671. Alpkem, Wilsonville, Oregon, USA.

———. 1992*c*. Nitrate + nitrite nitrogen. Document Number 000589. Alpkem, Wilsonville, Oregon, USA.

American Public Health Association. 1992. Standard methods for the examination of water and wastewater. Eighteenth edition. American Public Health Association, New York, New York, USA.

Bencala, K. E. 1993. A perspective on stream-catchment connections. Journal of North American Benthological Society **12**:4–47.

Blackmer, A. M., and J. M. Bremner. 1977. Nitrogen isotope discrimination in denitrification of nitrate in soils. Soil Biology and Biochemistry **9**:73–77.

Bowden, W. B., W. H. McDowell, C. E. Asbury, and A. M. Finley. 1992. Riparian nitrogen dynamics in two geomorphologically distinct tropical rain forest watersheds: nitrous oxide fluxes. Biogeochemistry **18**:77–99.

Bradley, P. M., M. Fernandez, Jr., and F. H. Chapelle. 1992. Carbon limitation of denitrification rates in an anaerobic groundwater system. Environmental Science and Technology **26**:2377–2381.

Bremner, J. M., and D. R. Keeney. 1966. Determination and isotope-ratio analysis of different forms of nitrogen in soils. 3. Exchangeable ammonium, nitrate and nitrite by extraction-distillation methods. Proceedings of Soil Science Society of America **30**:577–582.

Champ, D. R., J. Gulens, and R. E. Jackson. 1979. Oxidation-reduction sequences in ground water flow systems. Canadian Journal of Earth Sciences **16**:12–23.

Chapelle, F. H., and D. R. Lovely. 1992. Competitive exclusion of sulfate reduction by Fe(III)-reducing bacteria: a

mechanism for producing discrete zones of high-iron groundwater. Ground water **30**:29–36.

Cooper, A. B. 1990. Nitrate depletion in the riparian zone and stream channel of a small headwater catchment. Hydrobiologia **202**:13–26.

Correll, D. L. 1991. Human impact on the functioning of landscape boundaries. Pages 90–109 *in* M. M. Holland and R. J. Naiman, editors. Ecotones—the role of landscape boundaries in the management and restoration of changing environments. Chapman & Hall, New York, New York, USA.

Correll, D. L., and D. E. Weller. 1989. Factors limiting processes in freshwater wetlands: an agricultural primary stream riparian forest. Pages 9–23 *in* R. R. Sharitz and J. W. Gibbons, editors. Freshwater wetlands and wildlife conference. DOE Symposium Series number 8603101. U.S. Department of Energy, Washington, D.C., USA.

Dahm, C. N., D. L. Carr, and R. L. Coleman. 1991. Anaerobic carbon cycling in stream ecosystems. Internationale Vereinigung für Theoretischs and Angewandte Limnologie, Verhandlungen **24**:1600–1604.

D'Elia, C. F., P. A. Steudler, and N. Corwin. 1977. Determination of total nitrogen in aqueous samples using persulfate digestion. Limnology and Oceanography **22**:760–764.

Devito, K. J., P. J. Dillon, and B. D. Lazerte. 1989. Phosphorus and nitrogen retention in five Precambrian shield wetlands. Biogeochemistry **8**:185–204.

Findlay, S. 1995. Importance of surface–subsurface exchange in stream ecosystems: the hyporheic zone. Limnology and Oceanography **40**:159–164.

Firestone, M. K. and E. A. Davidson. 1989. Microbiological basis of NO and $N_2O$ production and consumption in soil. Pages 7–21 *in* M. O. Andreae, and D. S. Schimel, editors. Exchange of trace gases between terrestrial ecosystems and the atmosphere. Dahlem Konferenzen. John Wiley & Sons, Chichester, UK.

Freeze, R. A., and J. A. Cherry. 1979. Groundwater. Prentice-Hall, Englewood Cliffs, New Jersey, USA.

Grimm, N. B., and S. G. Fisher. 1984. Exchange between interstitial and surface water: implications for stream metabolism and nutrient cycling. Hydrobiologia **111**:219–228.

Groffman, P. M., E. A. Axelrod, J. L. Lemunyon, and W. M. Sullivan. 1991. Denitrification in grass and forest vegetated filter strips. Journal of Environmental Quality **20**:671–674.

Groffman, P. M., G. Howard, A. J. Gold, and W. M. Nelson. 1996. Microbial nitrate processing in shallow groundwater in a riparian forest. Journal of Environmental Quality **25**: 1309–1316.

Hanson, G. C., P. M. Groffman, and A. J. Gold. 1994. Symptoms of nitrogen saturation in a riparian wetland. Ecological Applications **4**:750–756.

Harvey, J. W., and K. E. Bencala. 1993. The effect of streambed topography on surface–subsurface water exchange in mountain catchments. Water Resources Research **29**:89–98.

Haycock, N. E., and G. Pinay. 1993. Groundwater nitrate dynamics in grass and poplar vegetated riparian buffer strips during the winter. Journal of Environmental Quality **22**:273–278.

Hendricks, S. P., and D. S. White. 1991. Physicochemical patterns within a hyporheic zone of a northern Michigan river, with comments on surface water patterns. Canadian Journal of Fisheries and Aquatic Sciences **48**:1645–1654.

Hedin, L. O. 1994. Stable isotopes, unstable forest. Nature **372**:725–726.

Hedin, L. O., and M. G. Brown. 1994. Watershed-level coupling of nitrogen and sulfur in a heterogeneous landscape. Internationale Vereinigung für Theoretische und Angewandte Limnologic, Verhandlungen **25**:1477–1482.

Hedin, L. O., G. E. Likens, K. M. Postek, and C. T. Driscoll. 1990. A field experiment to test whether organic acids buffer acid deposition. Nature **345**:798–800.

Hill, A. R. 1990. Ground water flow paths in relation to nitrogen chemistry in the near-stream zone. Hydrobiologia **206**:39–52.

———. 1991. A groundwater nitrogen budget for a headwater swamp in an area of permanent ground water discharge. Biogeochemistry **14**:209–224.

———. 1996. Nitrate removal in stream riparian zones. Journal of Environmental Quality **25**:743–754.

Hill, A. R., and J. M. Waddington. 1993. Analysis of storm run-off sources using oxygen-18 in a headwater swamp. Hydrological Processes **7**:305–316.

Holmes, R. M., S. G. Fisher, and N. B. Grimm. 1994. Parafluvial nitrogen dynamics in a desert stream ecosystem. Journal of North American Benthological Society **13**:468–478.

Howarth, R. W. 1993. Microbial processes in salt-marsh sediments. Pages 239–259 *in* T. E. Ford, editor. Aquatic microbiology: an ecological approach. Blackwell, Boston, Massachusetts, USA.

Howarth, R. W., G. Billen, D. Swaney, A. Townsend, N. Jaworski, K. Lajtha, J. A. Downing, R. Elmgren, N. Caraco, T. Jordan. F. Berendse, J. Freney, V. Kudeyarov, P. Murdoch, and Zhu Zhao-liang. 1996. Riverine inputs of nitrogen to the north Atlantic Ocean: fluxes and human influences. Biogeochemistry **35**:75–139.

Jacks, G., A. Joelsson, and S. Fleischer. 1994. Nitrogen retention in forested wetlands. Ambio **23**:358–362.

Jacobs, T. C., and J. W. Gilliam. 1985*a*. Headwater stream losses of nitrogen from two coastal plain watersheds. Journal of Environmental Quality **14**:467–472.

Jacobs, T. C., and J. W. Gilliam. 1985*b*. Riparian losses of nitrate from agricultural drainage waters. Journal of Environmental Quality **14**:472–478.

Jansson, M., R. Andersson, H. Berggren, and L. Leonardson. 1994. Wetlands and lakes as nitrogen traps. Ambio **23**: 320–325.

Jones, J. B., Jr. 1995. Factors controlling hyporheic respiration in a desert stream. Freshwater Biology **34**:91–99.

Jones, J. B., Jr, S. G. Fisher, and N. B. Grimm. 1995*a*. Nitrification in the hyporheic zone of a desert stream ecosystem. Journal of the North Americal Benthological Society **14**:249–258.

Jones, J. B., Jr, S. G. Fisher, and N. B. Grimm. 1995*b*. Vertical hydrologic exchange and ecosystem metabolism in a Sonoran Desert stream. Ecology **76**:942–952.

Jones, J. B., Jr., and R. M. Holmes. 1996. Surface–subsurface interactions in stream ecosystems. Trends in Ecology and Evolution **11**:239–242.

Jordan, T. E., D. L. Correll, and D. E. Weller. 1993. Nutrient interception by a riparian forest receiving inputs from adjacent croplant. Journal of Environmental Quality **22**:467–473.

Kristjansson, J. K., and P. Schönheit. 1983. Why do sulfate-reducing bacteria outcompete methanogenic bacteria for substrates? Oecologia **60**:264–266.

Likens, G. E., F. H. Bormann, R. S. Pierce, J. S. Eaton, and N. M. Johnson. 1977. Biogeochemistry of a forested ecosystem. Springer-Verlag, New York, New York, USA.

Lloyd, D. 1993. Aerobic denitrification in soils and sediments: from fallacies to facts. Trends in Ecology and Evolution **8**:352–356.

Lovely, D. R., and M. J. Klug. 1983. Sulfate reducers can outcompete methanogens at freshwater sulfate concentrations. Applied and Environmental Microbiology **45**:187–192.

Lovely, D. R., and E. J. P. Phillips. 1987. Competitive mechanisms for inhibition of sulfate reduction and methane production in the zone of ferric iron reduction in sediments. Applied and Environmental Microbiology **53**:2636–2641.

Lowrance, R. 1992. Groundwater nitrate and denitrification in a coastal plain riparian forest. Journal of Environmental Quality **21**:401–405.

Lowrance, R., L. S. Altier, J. D. Newbold, R. R. Schnabel, P. M. Groffman, J. M. Denver, D. L. Correll, J. W. Gilliam, J. L. Robinson, R. B. Brinsfield, K. W. Staver, W. Lucas, and A. H. Todd. 1995. Water quality functions of riparian forest buffer systems in the Chesapeake Bay Watershed. EPA 903-R-95-004. U.S. Environmental Protection Agency, Washington, D.C., USA.

Lowrance, R. R., R. L. Todd, and L. E. Asmussen. 1984*a*. Nutrient cycling in an agricultural watershed. I. Phreatic movement. Journal of Environmental Quality **13**:22–32.

Lowrance, R., R. Todd, J. Fail, O. J. Hendrickson, R. Leonard, and L. Asmussen. 1984*b*. Riparian forests as nutrient filters in agricultural watersheds. BioScience **34**:374–377.

Macko, S. A. 1981. Stable nitrogen isotope ratios as tracers of organic geochemical processes. Dissertation. University of Texas, Austin, Texas, USA.

Macko, S. A., and N. E. Ostrom. 1994. Pollution studies using stable isotopes. Pages 45–62 *in* K. Lajtha and R. Michner, editors. Stable isotopes in ecology and environmental science. Blackwell Scientific, Oxford, UK.

Matson, P. A., and P. M. Vitousek. 1995. Nitrogen trace gas emissions in a tropical dry forest ecosystem. Pages 384–398 *in* S. H. Bullock, H. A. Mooney, and E. Medina, editors. Seasonally dry tropical forests. Cambridge University Press, Cambridge, UK.

McClain, M. E., J. E. Richey, and T. P. Pimetel. 1994. Groundwater nitrogen dynamics at the terrestrial–lotic interface of a small catchment in the Central Amazon Basin. Biogeochemistry **27**:113–127.

McDowell, W. H., W. B. Bowden, and C. E. Asbury. 1992. Riparian nitrogen dynamics in two geomorphologically distinct tropical rain forest watersheds: subsurface and solute patterns. Biogeochemistry **18**:53–75.

McDowell, W. H., J. J. Cole, and C. T. Driscoll. 1987. Simplified version of the ampoule-persulfate method for determination of dissolved organic carbon. Canadian Journal of Fisheries and Aquatic Sciences **44**:214–218.

Morel, F. M. M., and J. G. Hering. 1993. Principles and applications of aquatic chemistry. John Wiley & Sons, New York, New York, USA.

Nadelhoffer, K. J., and B. Fry. 1994. Nitrogen isotope studies in forest ecosystems. Pages 22–44 *in* K. Lajtha, and R. Michner, editors. Stable isotopes in ecology and environmental science. Blackwell Scientific. Oxford, UK.

Paterson, K. G., and J. L. Schnoor. 1993. Vegetative alteration of nitrate fate in unsaturated zone. Journal of Environmental Engineering **119**:986–993.

Peterjohn, W. T., and D. L. Correll. 1984. Nutrient dynamics in an agricultural watershed: observations on the role of a riparian forest. Ecology **65**:1466–1475.

Phillips, P. J., J. M. Denver, R. J. Shedlock, and P. A. Hamilton. 1993. Effect of forested wetlands on nitrate concentrations in ground water and surface water on the Delmarva peninsula. Wetlands **13**:75–83.

Pickett, S. T. A., and M. L. Cadenasso. 1995. Landscape ecology: spatial heterogeneity in ecological systems. Science **269**:331–334.

Pinay, G., L. Roques, and A. Fabre. 1993. Spatial and temporal patterns of denitrification in a riparian forest. Journal of Applied Ecology **30**:581–591.

Pinay, G., C. Ruffinoni, and A. Fabre. 1995. Nitrogen cycling in two riparian forest soils under different geomorphic conditions. Biogeochemistry **30**:9–29.

Robinson, J. A., and J. M. Tiedje. 1984. Competition between sulfate-reducing and methanogenic bacteria for $H_2$ under resting and growing conditions. Oecologia **137**:26–32.

Sall, J., and A. Lehman. 1996. JMP Start statistics: a guide to statistics and data analysis using JMP and JMP IN software, Wadsworth, Belmont, California, USA.

Schipper, L. A., A. B. Cooper, C. G. Harfoot, and W. J. Dyck. 1993. Regulators of denitrification in an organic riparian soil. Soil Biology and Biochemistry **25**:925–933.

Simmons, R. C., A. J. Gold, and P. M. Groffman. 1992. Nitrate dynamics in riparian forests: groundwater studies. Journal of Environmental Quality **21**:656–665.

Snedecor, G. W., and W. G. Cochran. 1989. Statistical methods. Fifth edition. Iowa State University Press, Ames, Iowa, USA.

Smith, L., and S. W. Wheatcraft. 1993. Groundwater flow. Pages 6.1–6.58 *in* D. R. Maidment, editor. Handbook of hydrology. McGraw-Hill, New York, New York, USA.

Starr, R. C., and R. W. Gillham. 1993. Denitrification and organic carbon availability in two aquifers. Groundwater **31**:934–947.

Stumm, W., and J. J. Morgan. 1981. Aquatic chemistry: an introduction emphasizing chemical equilibria in natural waters. John Wiley & Sons, New York, New York, USA.

Tiedje, J. M. 1988. Ecology of denitrification and dissimilatory nitrate reduction to ammonium. Pages 179–244 *in* A. J. B. Zehnder, editor. Biology of anaerobic microorganisms. John Wiley & Sons, New York, New York, USA.

Triska, F. J., J. H. Duff, and R. J. Avanzino. 1993*a*. The role of water exchange between a stream channel and its hyporheic zone in nitrogen cycling at the terrestrial–aquatic interface. Hydrobiologia **251**:167–184.

Triska, F. J., J. H. Duff, and R. J. Avazino. 1993*b*. Patterns of hydrological exchange and nutrient transformation in the hyporheic zone of a gravel-bottom stream: examining terrestrial–aquatic linkages. Freshwater Biology **29**:259–274.

Valett, H. M., S. G. Fisher, N. B. Grimm, and P. Camill. 1994. Vertical hydrologic exchange and ecological stability of a desert stream. Ecology **75**:548–560.

Valett, H. M., J. A. Morrice, C. N. Dahm, and M. E. Campana. 1995. Parent lithology, surface–groundwater exchange, and nitrate retention in headwater streams. Limnology and Oceanography **41**:333–345.

Velinsky, D. J., J. R. Pennock, J. H. Sharp, L. A. Ciufuentes, and M. L. Fogel. 1989. Determination of the isotopic composition of ammonium-nitrogen at the natural abundance level from estuarine waters. Marine Chemistry **26**:351–361.

Vogel, J. C., A. S. Talma, and T. H. E. Heaton. 1981. Gaseous nitrogen as evidence for denitrification in groundwater. Journal of Hydrology **50**:191–200.

Vought, L., J. Dahl, C. Pedersen, and J. Pacoursiere. 1994. Nutrient retention in riparian ecotones. Ambio **23L**:342–348.

Warwick, J., and A. R. Hill. 1988. Nitrate depletion in the riparian zone of a small woodland stream. Hydrobiologia **157**:231–240.

Wetzel, R. G., and G. E. Likens. 1991. Limnological analyses. Springer-Verlag, New York, New York, USA.

Wilkinson, L. 1989. SYSTAT; The system for statistics. SYSTAT, Evanston, Illinois, USA.

Zehnder, A. J., and W. Stumm. 1988. Geochemistry and biogeochemistry of anaerobic habitats. Pages 1–38 *in* A. J. Zehnder, editor. Biology of anaerobic microorganisms. Wiley, New York.